Received: 13 December 2023 | Revised: 12 March 2024 | Accepted: 13 March 2024

DOI: 10.1002/alz.13828

Alzheimer's & Dementia®
THE JOURNAL OF THE ALZHEIMER'S ASSOCIATION

RESEARCH ARTICLE

Characterizing molecular and synaptic signatures in mouse models of late-onset Alzheimer's disease independent of amyloid and tau pathology

Kevin P. Kotredes[1] | Ravi S. Pandey[2] | Scott Persohn[3,4] | Kierra Elderidge[3,4] | Charles P Burton[3,4] | Ethan W. Miner[3,4] | Kathryn A. Haynes[5] | Diogo Francisco S. Santos[5] | Sean-Paul Williams[5] | Nicholas Heaton[5] | Cynthia M. Ingraham[4] | Christopher Lloyd[4] | Dylan Garceau[1] | Rita O'Rourke[1] | Sarah Herrick[1] | Claudia Rangel-Barajas[3,6] | Surendra Maharjan[3,4,7] | Nian Wang[3,4,7] | Michael Sasner[1] | Bruce T. Lamb[3,4,6] | Paul R. Territo[3,4,8] | Stacey J. Sukoff Rizzo[5] | Gregory W. Carter[1,2,9,10] | Gareth R. Howell[1,9,10] | Adrian L. Oblak[3,4,7]

[1]The Jackson Laboratory, Bar Harbor, Maine, USA

[2]The Jackson Laboratory for Genomic Medicine, Farmington, Connecticut, USA

[3]Indiana University School of Medicine, Indianapolis, Indiana, USA

[4]Stark Neurosciences Research Institute, Indianapolis, Indiana, USA

[5]Department of Medicine, University of Pittsburgh Aging Institute, University of Pittsburgh School of Medicine, Pittsburgh, Pennsylvania, USA

[6]Department of Medical and Molecular Genetics, Indiana University School of Medicine, Indianapolis, Indiana, USA

[7]Department of Radiology & Imaging Sciences, Indiana University School of Medicine, Indianapolis, Indiana, USA

[8]Department of Medicine, Division of Clinical Pharmacology, Indiana University School of Medicine, Indianapolis, Indiana, USA

[9]Tufts University Graduate School of Biomedical Sciences, Boston, Massachusetts, USA

[10]Graduate School of Biomedical Sciences and Engineering, University of Maine, Orono, Maine, USA

Correspondence
Gareth R. Howell, The Jackson Laboratory, Bar Harbor, ME, USA.
Email: gareth.howell@jax.org

Adrian L. Oblak, Indiana University School of Medicine, Indianapolis, IN, USA.
Email: aoblak@iupui.edu

Kevin P. Kotredes and Ravi S. Pandey are the co-first authors.

Abstract

INTRODUCTION: MODEL-AD (Model Organism Development and Evaluation for Late-Onset Alzheimer's Disease) is creating and distributing novel mouse models with humanized, clinically relevant genetic risk factors to capture the trajectory and progression of late-onset Alzheimer's disease (LOAD) more accurately.

METHODS: We created the LOAD2 model by combining apolipoprotein E4 (APOE4), Trem2*R47H, and humanized amyloid-beta (Aβ). Mice were subjected to a control diet

Funding information: Rush Alzheimer's Disease Center, Rush University Medical Center, Chicago; NIA, Grant/Award Numbers: P30AG10161, R01AG15819, R01AG17917, R01AG36836, U54AG054345, P50 AG016574, R01 AG032990, U01 AG046139, R01 AG018023, U01 AG006576, U01 AG006786, R01 AG025711, R01 AG017216, R01 AG003949, P30 AG19610; Illinois Department of Public Health (ROSMAP); Translational Genomics Research Institute; NINDS, Grant/Award Numbers: R01 NS080820, U24 NS072026, R01NS125020; CurePSP Foundation; Mayo Foundation; National Brain and Tissue Resource for Parkinson's Disease and Related Disorders; Arizona Alzheimer's Disease Core Center; Arizona Department of Health Services; Arizona Alzheimer's Research Center; Arizona Biomedical Research Commission; Arizona Parkinson's Disease Consortium; Michael J. Fox Foundation for Parkinson's Research; Diana Davis Spencer Endowed Chair Research; Bernard and Lusia Milch Endowed Chair

This is an open access article under the terms of the Creative Commons Attribution-NonCommercial-NoDerivs License, which permits use and distribution in any medium, provided the original work is properly cited, the use is non-commercial and no modifications or adaptations are made.
© 2024 The Authors. *Alzheimer's & Dementia* published by Wiley Periodicals LLC on behalf of Alzheimer's Association.

or a high-fat/high-sugar diet (LOAD2+HFD). We assessed disease-relevant outcome measures in plasma and brain including neuroinflammation, Aβ, neurodegeneration, neuroimaging, and multi-omics.

RESULTS: By 18 months, LOAD2+HFD mice exhibited sex-specific neuron loss, elevated insoluble brain Aβ42, increased plasma neurofilament light chain (NfL), and altered gene/protein expression related to lipid metabolism and synaptic function. Imaging showed reductions in brain volume and neurovascular uncoupling. Deficits in acquiring touchscreen-based cognitive tasks were observed.

DISCUSSION: The comprehensive characterization of LOAD2+HFD mice reveals that this model is important for preclinical studies seeking to understand disease trajectory and progression of LOAD prior to or independent of amyloid plaques and tau tangles.

KEYWORDS
Alzheimer's disease, APOE4, genetics, high-fat diet, late-onset Alzheimer's disease, LOAD, MODEL-AD, TREM2

Highlights

- By 18 months, unlike control mice (e.g., LOAD2 mice fed a control diet, CD), LOAD2+HFD mice presented subtle but significant loss of neurons in the cortex, elevated levels of insoluble Ab42 in the brain, and increased plasma neurofilament light chain (NfL).
- Transcriptomics and proteomics showed changes in gene/proteins relating to a variety of disease-relevant processes including lipid metabolism and synaptic function.
- In vivo imaging revealed an age-dependent reduction in brain region volume (MRI) and neurovascular uncoupling (PET/CT).
- LOAD2+HFD mice also demonstrated deficits in acquisition of touchscreen-based cognitive tasks.

1 | BACKGROUND

Late-onset Alzheimer's disease (LOAD) is the most common form of dementia, caused by a combination of genetic and environmental factors.[1–3] Despite the recent approval of anti-amyloid therapies such as Aduhelm[4] and Leqembi,[5] additional therapeutic options are essential to prevent or slow cognitive decline in most cases of LOAD. To achieve this, preclinical models that more faithfully reproduce the complex features of LOAD as well as the long prodromal period and slow progression through aging, are required to identify targets that precede the onset of frank neuropathology that are tractable for intervention.

While hundreds of preclinical models are available that represent stages of disease with significant amyloid and tau accumulation, some with robust behavioral changes (although disease relevance is questionable), but most with no frank neurodegeneration, the field has been challenged by the lack of models that recapitulate the early prodromal period of disease in which gene expression changes herald the onset of the beginning of toxic pathologies and mild cognitive impairment is diagnosed. This is more in line with the sporadic, late-onset form of AD that will impact 95% of individuals diagnosed with AD, versus the 5% of familial AD cases that have been modeled and studied historically with mouse models to date. The MODEL-AD (Model Organism Development and Evaluation for Late-Onset Alzheimer's disease) consortium is charged with creating and phenotyping new mouse models based on the genetics of LOAD.[6] The IU/JAX/PITT MODEL-AD Center has focused on creating models on the C57BL/6J (B6J) genetic background that incorporate the e4 allele of the apolipoprotein E gene (*APOE4*),[7] the greatest genetic risk factor for LOAD. In addition, we created the e3 (neutral) allele (*APOE3*).[7] These humanized APOE alleles allow for unrestricted use and breeding that was not readily available with previous versions.[7] This allowed us to determine the effects of combining multiple genetic risk factors for LOAD. We generated and characterized B6J mice that were double homozygous for both *APOE4* and the *R47H* variant in *Trem2* (Triggering receptor expressed on myeloid cells 2). These mice were termed LOAD1.[8] Although LOAD1 mice did not

develop classic hallmarks of LOAD, such as amyloid pathology, neurodegeneration, and cognitive decline, they did show alterations in gene expression levels in the brain similar to those seen in LOAD patients, as well as changes in cerebrovascular blood flow and glucose uptake.[8]

We now present the comprehensive characterization of LOAD2 (B6J.*APOE4.Trem2*R47H.hAβ* triple homozygous), where the amyloid-beta (Aβ) sequence of the mouse *App* gene of LOAD1 mice has been humanized.[8] Data support that the human Aβ sequence is more amyloidogenic than the mouse version, so we tested the hypothesis that LOAD2 mice will develop features of LOAD that were absent in LOAD1 mice. In addition, we evaluate a high-fat diet/high-sugar diet (HFD), a common environmental stressor, which human and mouse studies show increases the risk for LOAD.[9,10] For instance, our previous study showed chronic consumption of a HFD exacerbated the genetic effects of LOAD1 mice carrying the *Plcg2*M28L*[10] *variant*. Here, using a combination of a cross-sectional and longitudinal design, cohorts of male and female LOAD1 and LOAD2 mice were fed either a control diet (CD) or HFD from 2 months of age and evaluated at 4, 12, 18, or 24 months of age. Data show that, unlike LOAD1 mice, LOAD2 mice conditioned on a HFD (LOAD2+HFD) resulted in age-related, and in some cases sex-specific, neurodegeneration, cognitive deficits, elevations in insoluble Aβ, LOAD-relevant imaging abnormalities, and increased neurofilament light chain (NfL) in the plasma. These phenotypes are consistent with endophenotypes observed in the earliest stages of LOAD prior to significant neuropathology and cognitive decline. We propose LOAD2+HFD as a complementary model to existing models of amyloid and tau pathology, a mouse model for investigating therapeutic interventions independent of targeting amyloid and tau pathologies, and importantly prior to significant pathology in the brain which is the treatment paradigm (prophylactic) most needed in the field in order to prevent AD.

RESEARCH IN CONTEXT

1. **Systematic review**: The authors reviewed the literature using PubMed. Late-onset Alzheimer's disease (LOAD) is a complex neurodegenerative disorder influenced by a combination of genetic and environmental factors.
2. **Interpretation**: Results at 18 months revealed distinctive characteristics in LOAD2+HFD (high-fat/high-sugar diet) mice compared to control mice, which included subtle but significant neuronal loss in the cortex, elevated levels of insoluble amyloid-beta (Aβ) 42 in the brain, and increased plasma neurofilament light chain (NfL). Transcriptomic and proteomic analyses indicated alterations in genes and proteins associated with various disease-relevant processes, such as lipid metabolism and synaptic function. In vivo imaging demonstrated age-dependent reductions in brain region volume and neurovascular uncoupling. Notably, despite the absence of hallmark amyloid and Tau pathologies, LOAD2+HFD mice exhibited learning deficits in touchscreen-based cognitive tasks.
3. **Future directions**: The findings collectively suggest that the LOAD2+HFD mouse model provides a valuable platform for preclinical studies, particularly for investigating aspects of LOAD independent of amyloid and tau pathologies.

2 | METHODS

LOAD2 mice were created at JAX and distributed to IU and PITT for evaluation and cross-laboratory reproducibility of LOAD-relevant phenotypes using the IU/JAX/PITT MODEL-AD center pipeline that includes a combination of human-relevant in vivo and *post mortem* assays. The primary goal of the phenotyping pipeline is to determine the utility of new LOAD models for preclinical testing, with a particular focus on identifying targets early in the long prodromal stages of disease prior to significant pathology or significant decline in cognitive function. Five cohorts of LOAD2 and control mice fed either a HFD (high-fat diet) or CD (control diet) were evaluated at JAX (Cohort 1: biometrics, behavior, plasma biomarkers, neuropathology, transcriptomics, proteomics), IU (Cohort 2: MRI, plasma biomarkers and cytokines, biochemistry, neuropathology; Cohort 3: PET/CT, autoradiography), and PITT (Cohorts 4 and 5: longitudinal plasma biomarkers, Touchscreen cognitive testing) (Figure S1). Unless otherwise stated, to evaluate LOAD2 phenotypes (on CD or HFD), LOAD1 mice were used as the control genotype to evaluate the effects of humanizing the Aβ sequence in the context of the *APOE4* and Trem2*R47H risk alleles (LOAD1). LOAD1 and LOAD2 mice both express humanized *APOE4* and *Trem2*R47H risk* alleles on a B6J background, however LOAD2 animals also express a humanized allele for *App* (Figure 1A).

2.1 | Creation of the humanized Aβ allele

The humanized Aβ allele was created by direct delivery of CRISPR-Cas9 reagents to mouse zygotes of the APOE4/Trem2*R47H model, (B6(SJL)-*Apoe*$^{tm1.1(APOE*4)Adiuj}$ *Trem2*^{em1Adiuj}/J, or "LOAD1," JAX #28709, https://www.jax.org/strain/028709), which was previously described.[8]

Analysis of genomic DNA sequence surrounding the target region, using the Benchling (www.benchling.com) guide RNA design tool, identified a gRNA sequence (TTTGATGGCGGACTTCAAATC) with a suitable target endonuclease site in exon 14 of the mouse App locus. Streptococcus pyogenes Cas9 (SpCas9) V3 protein and gRNA were purchased as part of the Alt-R CRISPR-Cas9 system using the crRNA:tracrRNA duplex format as the gRNA species (IDT, USA). Alt-R CRISPR-Cas9 crRNAs (Product# 1072532, IDT, USA) were synthesized using the gRNA sequences specified in the DESIGN section and hybridized with the Alt-R tracrRNA (Product# 1072534, IDT, USA) as per manufacturer's instructions.

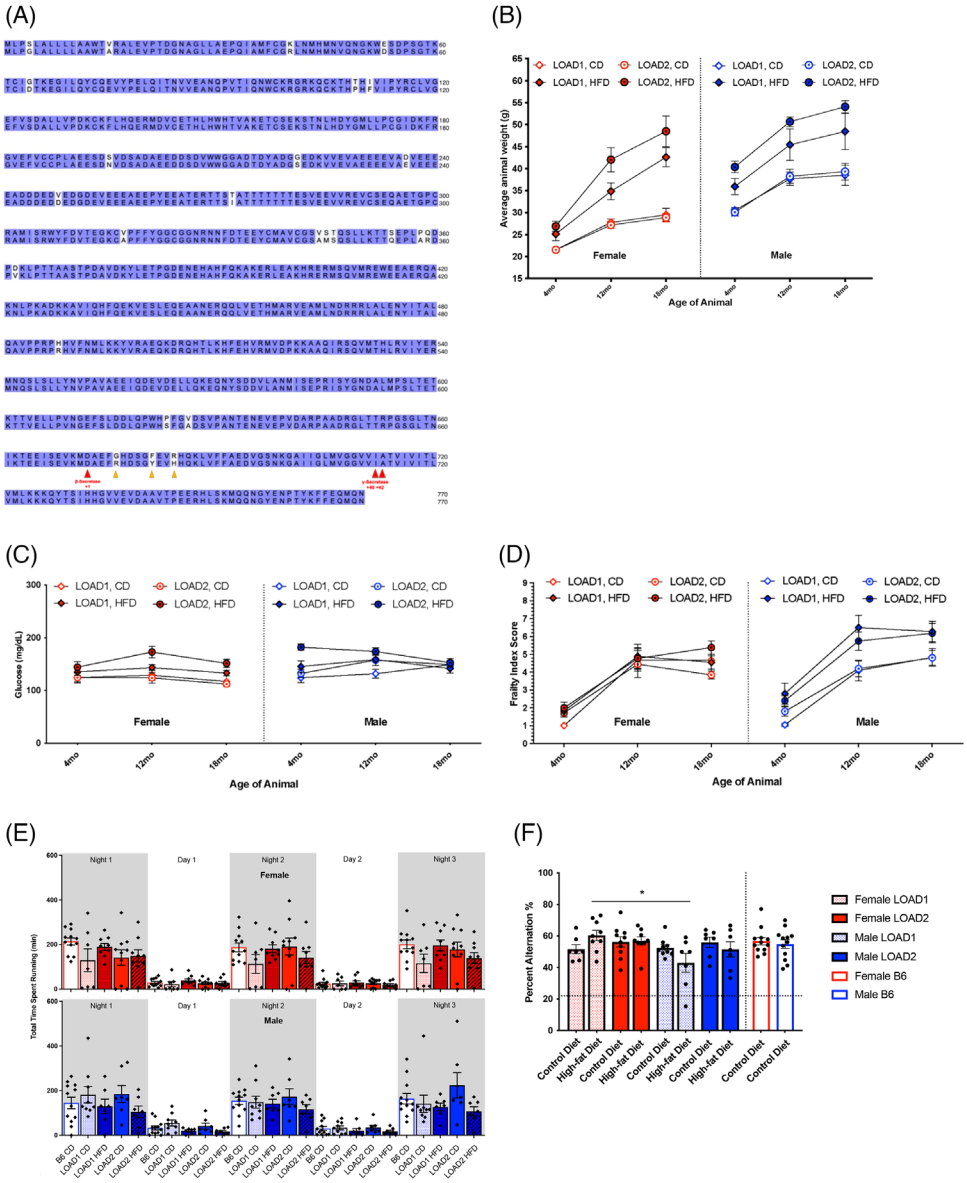

FIGURE 1 Longitudinal metabolic and behavioral phenotyping of mice on high-fat diet. LOAD1 (*APOE4/Trem2*R47H*) and LOAD2 (*hAbeta/APOE4/Trem2*R47H*) animal strains differ in the *App* allele with a humanized Abeta1-42 region (G601R, F606Y, R609H in the mouse gene, corresponding to amino acid positions 676, 681, 684 in the human *APP* locus) (A). Alignment of mouse (top; Uniprot ID P12023) and humanized (bottom; Uniprot ID P05067) APP amino acid sequences. White letters denote nonhomology. Red arrows indicate cleavage sites of processing enzymes. Yellow arrows denote sites of humanizing mutations in *App* allele (LOAD1, top, and LOAD2, bottom). (Cohort 1) Animals of an 18 month longitudinal cohort were assayed at 4, 12, and 18 months of age. Males and females, of LOAD1 and LOAD2 genotypes, fed either CD or HFD beginning at 2-months of age were measured for body weight (B), fasted blood glucose (C), and frailty assay index score (D), as a measure of general animal health changes. Running wheel assay measured average animal activity time for 3 days and nights at the 18 month age timepoint (E). Spontaneous alternation behavioral assay was utilized to measure cognition longitudinally across ages at the 18-month age timepoint (F) (Three-way ANOVA [sex, genotype, diet effects]; * = $p < 0.05$). APP, amyloid precursor protein; CD, control diet; HFD, high-fat diet.

A single-stranded DNA repair construct (synthesized by Genscript) with the sequence 5′-CTGGGCTGACAAACATCAAGACGGA AGAGATCTCGGAAGTGAAGATGGATGCAGAATTC**C**GACATGATT CAGGAT**A**TGAAGTCC**AT**CATCAAAAACTGGTAGGCAAAAATAAAC TGCCTCTCCCCGAGATTGCGTCTGGCCAGATGAAAT-3′ was used to introduce the G601R, F606Y, and R609H amino acid changes in the mouse *App* sequence (corresponding to G676R, F681Y, and R864H in human *APP*) such that the Ab-42 region matches the human sequence (Figure 1A).

Founders were bred to the LOAD1 model and genotyped for the humanized Aβ locus by polymerase chain reaction (PCR) using forward primer 5′-CAGTTTTTGCCTCCTTGTGG-3′ and reverse primer 5′-GGCTTCTGCTCAGCAAGAACTA-3′. A positive reaction was determined by the presence of a band of 362 bp. The resulting strain

("LOAD2") is available as JAX #30670, B6J.Cg-*Apoe*$^{tm1.1(APOE*4)Adiuj}$ *App*^{em1Adiuj} *Trem2*^{em1Adiuj}/J (https://www.jax.org/strain/030670; B6J.*APOE*$^{E4/E4}$.*Trem2*$^{R47H/R47H}$.*App*$^{hA\beta/hA\beta}$). The *App* allele alone is available as JAX #33013, B6J.Cg-*App*^{em1Adiuj}/J (https://www.jax.org/strain/033013).

2.2 | Cohort generation and evaluation

To evaluate LOAD-relevant phenotypes, five cohorts of LOAD2 mice and controls were created at The Jackson Laboratory (JAX, cohort 1), Indiana University (IU, cohorts 2 and 3) and University of Pittsburgh (PITT, cohorts 4 and 5). Breeding, mouse husbandry, and assays common across sites were standardized as much as possible. Below, we provide brief details of each cohort and assays performed with full details included provided in Supplemental Methods.

2.2.1 | Cohort 1: The Jackson Laboratory

All procedures were approved by The Jackson Laboratory Institutional Animal Care and Use Committee (IACUC).

Experimental groups

To create experimental groups, B6J.*APOE*$^{E4/E4}$.*Trem2*$^{R47H/R47H}$.*App*$^{hA\beta/+}$ mice were intercrossed to create B6J.*APOE*$^{E4/E4}$.*Trem2*$^{R47H/R47H}$.*App*$^{hA\beta/hA\beta}$ (LOAD2) and B6J.*APOE*$^{E4/E4}$.*Trem2*$^{R47H/R47H}$.*App*$^{+/+}$ (LOAD1) control mice. In appreciation of sexual dimorphism observed in human aging and disease, four groups of male and female mice were established for a combination of longitudinal and cross-sectional phenotyping at 4, 12, 18, and 24 months. The 18 month group was assessed for biometrics and plasma biomarkers at 4, 8, 12, and 18 months.

All mice were initially provided LabDiet 5K52/5K67 (6% fat; control diet, CD). At 2 months of age, each experimental group was randomized into two groups, the control group, and the high-fat diet (HFD) group. The control groups continued on CD ad libitum, while the HFD groups were provided ResearchDiet feed D12451i (45% high fat, 35% carbohydrates) ad libitum. Due to attrition between 18 and 24 months of age, the 24-month HFD cohort was not sufficiently powered and so not analyzed. For in vivo studies—at least 10 mice/sex/genotype/age/diet were evaluated. For *post mortem* analyses, 6 mice/sex/genotype/age/diet were evaluated unless otherwise stated.

Phenotyping

The cross-sectional phenotyping battery included in vivo frailty, behavioral phenotyping, with metabolic profiling and biomarker (e.g., neurofilament light chain, NfL) analyses in the plasma. *Post mortem* brain tissue was examined for transcriptomic and proteomic analyses as well as neuropathological indications of disease (amyloid, neuronal cell loss, and glial activation). For full details see Supplemental Methods (Figure S1).

2.2.2 | Cohorts 2: Indiana University

All procedures were approved by the Indiana University Institutional Animal Care and Use Committee (IACUC). The same bedding, light cycle, and water conditions as The Jackson Laboratory were used at Indiana University.

Experimental groups

LOAD2 mice were imported from JAX and bred at IU. LOAD2 mice were initially crossed to LOAD1 mice to create B6J.*APOE*$^{E4/E4}$.*Trem2*$^{R47H/R47H}$.*App*$^{hA\beta/+}$ mice which were then intercrossed to create B6J.*APOE*$^{E4/E4}$.*Trem2*$^{R47H/R47H}$.*App*$^{hA\beta/hA\beta}$ (LOAD2) mice. One group of at least 10 male and 10 female mice were established for longitudinal phenotyping at 4, 12, and 18 months. Similar to the JAX cohort, mice were initially provided CD before half the mice in each group were switched to HFD.

Phenotyping

At 4, 12, and 18 months, mice underwent in vivo MR imaging (T2 weighted images) and blood draws for biomarker (e.g., Aβ species, cytokines) analyses. For full details, see Supplemental Methods. At 18 months, tissues were collected as described for Cohort 1.

2.2.3 | Cohort 3: Indiana University

All procedures were approved by the Indiana University Institutional Animal Care and Use Committee (IACUC). The same bedding, light cycle, and water conditions as The Jackson Laboratory were used at Indiana University.

Experimental groups

Experimental groups of male and female LOAD2 mice on HFD or CD were established as described for Cohort 3 (n = 12 mice/sex/genotype/age/diet). Three groups were established for cross-sectional analyses at 4, 12, and 18 months.

Phenotyping

To evaluate neurovascular uncoupling, in vivo PET/CT imaging was performed on all mice measuring regional blood flow (via ^{64}Cu-pyruvaldehyde-bis(N4-methylthiosemicarbazone, ^{64}Cu-PTSM) and regional glycolytic metabolism (via 2-^{18}F-2-deoxyglucose, ^{18}F-FDG). Findings from in vivo PET/CT were confirmed using autoradiography. For full details, see Supplemental Methods.

2.2.4 | Cohort 4 and 5: University of Pittsburgh

All procedures were approved by the University of Pittsburgh Institutional Animal Care and Use Committee (IACUC). Detailed mouse husbandry, diet restriction, and phenotyping methods are included in the Supplemental Methods.

Experimental groups

Two experimental cohorts were evaluated for plasma biomarkers and cognitive testing. Breeding pairs of LOAD2 mice were imported from JAX and bred at the University of Pittsburgh to create Cohort 4. One group of n = 18 male and n = 18 female mice were established for longitudinal blood plasma collection followed by cognitive assessments using the touchscreen. Subjects were reared on normal control diet (CD) (LabDiet 5P76) provided ad libitum until 2 months of age at which time n = 13 male and n = 14 female mice were randomly assigned to receive ad libitum HFD (LOAD2+HFD). For cohort 5, LOAD2 mice (B6J.*APOE*$^{E4/E4}$.*Trem2*$^{R47H/R47H}$.*App*$^{hA\beta/hA\beta}$) were back-crossed by breeding with C57BL/6J to provide littermate controls. The F1 offspring which were triple heterozygotes (B6J.*APOE*$^{E4/+}$.*Trem2*$^{R47H/+}$.*App*$^{hA\beta/+}$) were then crossbred to produce F2 offspring including the LOAD2 triple homozygote mice (n = 9/sex) and triple wild-type (WT) littermate controls (n = 6/sex). All mice were initially reared on CD, with n = 3/sex WT controls and n = 6/sex LOAD2 switched to ad libitum HFD at 6–12 months of age. Prior to touchscreen testing, mice were individually housed and restricted to 80%–85% of free-feeding body weight. Mice were weighed daily and provided a ration of the respective CD or HFD diets that maintained them at 80%–85% restriction.

Phenotyping

Plasma was measured longitudinally prior to the start of HFD, followed monthly for analysis of cytokines and every 3 months for analysis of Aβ species. To evaluate the effect of food restriction on plasma biomarker levels, brief 2-week periods of food restriction as described above were administered to Cohort 4 at 8–8.5 months of age and at 10–10.5 months of age. At 14 months of age, Cohort 4 was enrolled in Touchscreen cognitive testing and maintained continuously on dietary restriction until the conclusion of touchscreen testing; while Cohort 5 began food restriction and touchscreen testing at 11–17 months of age.

3 | RESULTS

3.1 | Aging × LOAD genetic risk × environment demonstrate diet- and age-dependent neuronal phenotypes in LOAD2+HFD mice

We first evaluated the 18 month aged LOAD2 mice using in vivo assays following a longitudinal design. Longitudinal testing and sampling were performed at 4, 12, and 18 months of age. We observed significant, HFD-driven increases in body weight with age (Figure 1B). All mice showed an increase in weight with age, but mice fed HFD showed pronounced weight gain until 18 months of age. Females on the HFD displayed significant weight gain from 4 to 12 months, but only made modest gains from 12 to 18 months. Males fed a HFD were more accelerated than females, and LOAD2 males were consistently heavier than LOAD1 males at all timepoints. However, fasted blood glucose measurements did not appear to be age-, diet-, or genotype-dependent, though slightly elevated levels were observed in LOAD2 mice fed HFD (LOAD2+HFD) (Figure 1C). As expected, age was a strong factor of increased frailty[11] (Figure 1D). However, we did not see significant diet-related changes in frailty scores in females until 18 months of age and only in LOAD2 genotype animals. Males consistently displayed increased frailty driven by diet, but not genotype, as early as 8 months of age (data not shown).

HFD altered performance in open field assays compared to CD. Specifically, total distance traveled decreased significantly only in LOAD2+HFD animals (Figure S2A), but performance was not affected by sex or genotype alone. Differences in rearing behavior as measured by total vertical activity were only observed in males, of both genotypes, to be decreased by HFD (Figure S2B). Rotarod performance was decreased in a HFD-dependent manner only (Figure S2C). LOAD2+HFD animals, however, particularly males, demonstrated a reduction in running wheel activity during the active period (dark cycle) compared to LOAD1 mice or those fed CD (Figure 1E). Hippocampal working memory in the spontaneous alternation assay as a measure of cognitive function was intact across all groups with all subjects performing > chance levels which is calculated as 22% in this assay (Figure 1F).

Brains from mice from the 18 month group were harvested (along with the 4, 12, and 24 month groups). One hemisphere (right) from each brain was prepared for transcriptomics and proteomics, while the other hemisphere (left) was evaluated for neuronal cell loss, microglia number, astrocyte reactivity, and amyloid plaques in the cortex and hippocampus by immunofluorescence (Figure S3). At 18 months of age, neuron counts in the cortex revealed a subtle but statistically significant decrease in NeuN+DAPI+ cells in female LOAD2+HFD compared to female LOAD2+CD and female LOAD1+HFD (Figure 2A,B). No differences were observed in cortical IBA1+DAPI+ microglia number (Figure 2C,D) across all groups, and a small but significant decrease in hippocampal astrocyte reactivity (assessed using GFAP+DAPI+) in male LOAD2+HFD mice compared to those fed a CD diet (Figure 2E,F). ThioS staining revealed no evidence of amyloid plaques in any groups (Figure 2G). To determine whether neuronal cell changes in LOAD2+HFD was reflected by changes in the plasma, NFL, a clinically relevant biomarker[12] was assessed. Linear modeling of plasma NfL levels revealed significant increases in LOAD2 animals on both diets (Figure 2H). Similarly, we saw a significant increase in LOAD1+HFD relative to LOAD1+CD. These data indicate a relationship of neuronal loss with impaired behavioral function that is exacerbated in aged mice with LOAD genetic risk in the context of environmental stressor of HFD.

3.2 | Transcriptional analysis of aging × LOAD genetic risk × environment reveals differential effects of sex changes

To identify molecular effects of humanizing the Aβ peptide, we first performed pairwise differential analysis between LOAD2 and LOAD1 mice at all ages for both sexes. Differential expression analyses identified very few significantly differentially expressed genes (DEGs) (p < 0.05) at 4 and 18 month old LOAD2 mice compared to age- and sex-matched LOAD1 mice (Table SA). At 12 months,

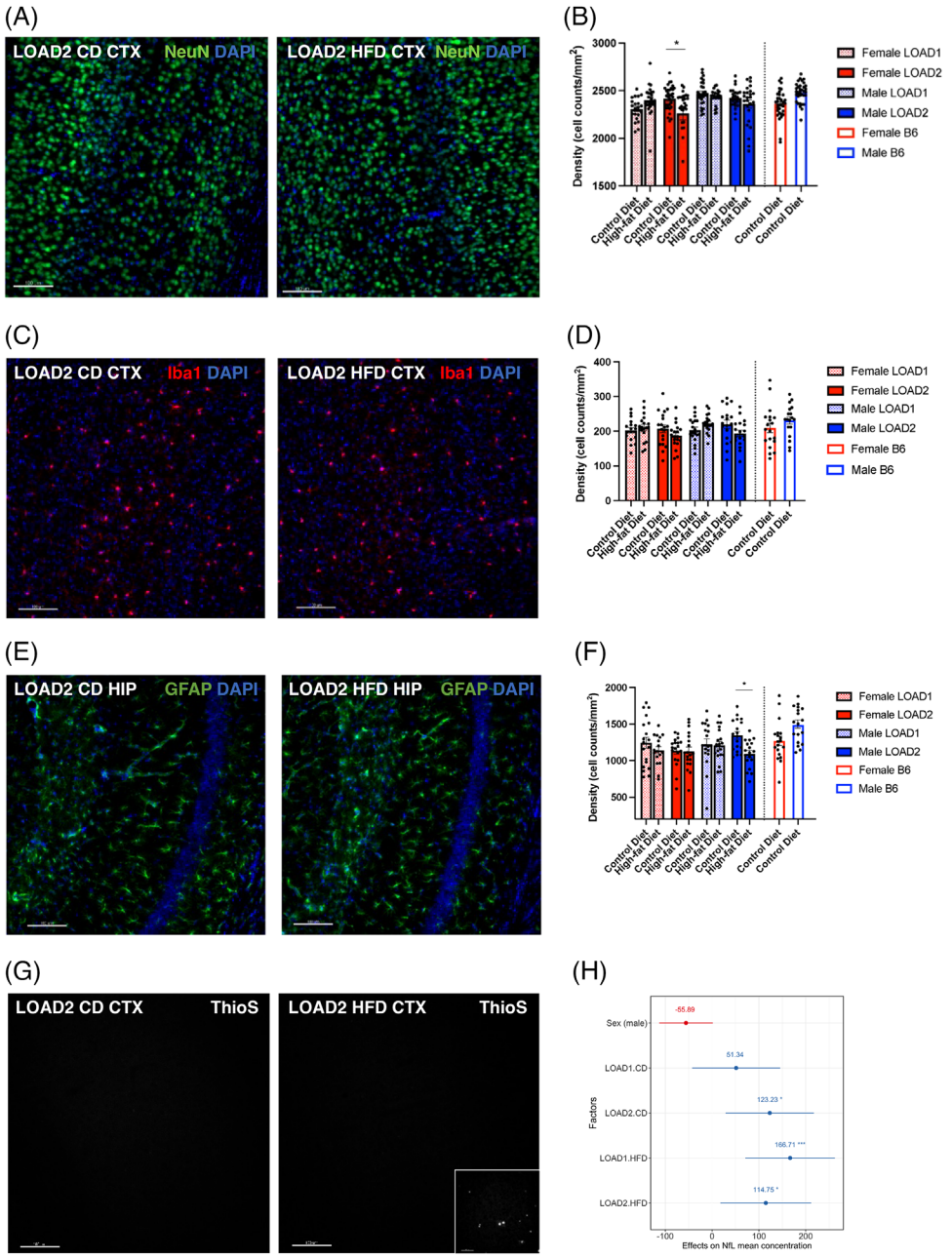

FIGURE 2 Neuropathological assessment of brain tissue. Immunohistochemistry of brain tissue in the cortex and hippocampus from 18 month old animals stained for cell markers to reveal genotype- and diet-driven differences in glial cell densities. Slices of brain hemispheres were stained with NeuN (neurons A,B) or IBA1 (microglia C,D) (representative cortical images shown from LOAD2 females with DAPI co-stain) and counted relative to area. Astrocytes (GFAP) quantitated in the hippocampus of LOAD2 females fed either CD or HFD (E-F). ThioS staining of brain tissue to visualize amyloid plaques (representative images shown from LOAD2 females) (G). Inlay: scaled image of 12 month B6J.*APP-SAA* hyperamyloid positive controls. Linear regression analyses were performed to identify effect of each factor on neurofilament light-chain (NfL) levels determined by ELISA testing in plasma derived from terminal, peripheral blood samples at 18 months of age (H). (NeuN = neuronal marker; ThioS = amyloid plaques; GFAP = astrocyte marker; IBA1 = microglial marker. Scale bar equals 100 μm).

there were 57 DEGs (38 upregulated, 19 downregulated; $p < 0.05$) in male LOAD2 mice, and 17 DEGs (3 upregulated, 14 downregulated; $p < 0.05$) in female LOAD2 mice (Table SA). KEGG functional enrichment analysis identified enrichment of "protein processing in ER" in upregulated DEGs in 12 month old LOAD2 male mice and "MAPK signaling pathway" in downregulated DEGs in 12 month old LOAD2 female mice (Table SB). At 24 months, there were only five significantly differentially upregulated genes ($p < 0.05$) in male LOAD2 mice, and 30 DEGs (12 upregulated, 18 downregulated; $p < 0.05$) in female LOAD2 mice (Table SA). Upregulated DEGs in male and female LOAD2 mice were enriched for the "motor proteins" KEGG pathways (Table SB).

Next, we performed differential analyses in 18 month old LOAD2 and LOAD1 mice compared to age and sex-matched B6J control mice. In females, we observed only 9 significant DEGs (3 upregulated, 6 downregulated) ($p < 0.05$) in LOAD2 mice on control diet (CD), while 2988 genes were significantly differentially expressed (1565 upregulated, 1423 downregulated) ($p < 0.05$) in LOAD2+HFD (Table SA). We observed 44 significantly DEGs (19 upregulated, 25 downregulated) ($p < 0.05$) in female LOAD1+CD, while 164 genes were significantly differentially expressed (117 upregulated, 47 downregulated) ($p < 0.05$) in female LOAD1+HFD (Table SA). In males, we observed a total of 7 and 23 significant DEGs ($p < 0.05$) in LOAD1 and LOAD2 mice on CD, respectively, while 39 and 98 genes were significantly expressed ($p < 0.05$) in LOAD1 and LOAD2 mice on HFD, respectively (Table SA). Overall, we observed more differentially expressed genes in mice conditioned on HFD, and this effect was more prominent in female mice expressing humanized Aβ.

Functional enrichment analyses of DEGs in female LOAD2+HFD identified enrichment of multiple KEGG pathways such as "glutamatergic synapse," "dopaminergic synapse," and "MAPK signaling pathway" in upregulated genes, while downregulated genes were enriched for KEGG pathways such as "lysosome," "fatty acid metabolism," "TCS cycle," and "valine, leucine and isoleucine degradation." Differentially upregulated genes in female LOAD1+HFD were enriched for "circadian entrainment," while downregulated genes were enriched for "phagosome" KEGG pathway (Table SB). We did not observe enrichment for any KEGG pathways in DEGs in LOAD1 and LOAD2 mice on control diet.

Next, we assess the effect of HFD by performing differential analysis between mice fed the HFD with age, sex, and genotype-matched mice on CD. We observed 260 significant DEGs (154 upregulated, 106 downregulated) ($p < 0.05$) in female LOAD2+HFD compared to female LOAD2+CD, while 45 significant DEGs (9 upregulated, 36 downregulated) ($p < 0.05$) in male LOAD2+HFD compared to male LOAD2+CD (Table SA). In LOAD1 male mice, we observed a total of 12 DEGs ($p < 0.05$) on HFD compared to CD, while only two DEGs ($p < 0.05$) on HFD compared to CD in female LOAD1 mice (Table SA). Upregulated genes in female LOAD2 female mice on HFD compared to CD were enriched for KEGG pathways such as "glutamatergic synapse," "dopaminergic synapse," and "MAPK signaling pathway," while downregulated genes in female LOAD2+HFD compared to CD were enriched for "motor proteins" pathway (Table SB).

3.2.1 | Gene modules associated with AD pathology driven by age and high-fat high-sugar diet

Differential expression analyses identified subtle changes at the gene level and suggested pronounced effect of LOAD2 genotype by high-fat/high-sugar diet (HFD) in aged mice. To further ensure these signals, we performed a weighted gene co-expression network analysis (WGCNA)[13] on the brain transcriptome to identify gene expression changes in a system-level framework. WGCNA identified 30 distinct modules of co-expressed genes (Table SB2).

To understand the functional significance of these modules, we correlated each module eigengene with age, sex, diet, genotype, and measured behavioral assays such as cumulative frailty score, body weights, NfL, plasma cytokines, GFAP, Iba1, and NeuN counts (Figure S4). Eighteen of these 30 modules were significantly correlated with age ($p < 0.05$) (turquoise, lightyellow, darkgreen, green, darkgray, floralwhite, purple, brown4, red, skyblue3, lightcyan, orangred4, darkorange2, plum1, orange, lightcyan1, greenyellow, and blue). Six modules were significantly correlated with HFD ($p < 0.05$) (lightyellow, turquoise, brown4, darkgray, darkred, orangered4). Seven modules were significantly correlated with sex ($p < 0.05$) (sienna3, greenyellow, orangered4, darkmagenta, skyblue3, red, bisque4). Two modules (greenyellow and sienna3) were significantly correlated with the Apoe4.Trem2*R47H allele combination in both LOAD1 and LOAD2 ($p < 0.05$), while five modules were significantly correlated with humanized Aβ specific to LOAD2 ($p < 0.05$) (brown, thistle3, greenyellow, blue, and orange) (Figure S4).

We observed that HFD was strongly significantly correlated with the lightyellow module ($r = 0.45$; $p = 9 \times 10^{-9}$), while age was strongly significantly correlated with both the turquoise ($r = 0.81$; $p = 2 \times 10^{-35}$) and lightyellow modules ($r = 0.52$; $p = 1 \times 10^{-11}$) (Figure S4).

To further elucidate the association of the lightyellow and turquoise modules with age, sex, and genotype-diet combinations, we performed linear regression analysis using module eigengene as the dependent variable. We determined that the lightyellow module was significantly positively correlated with LOAD1 and LOAD2 genotype with HFD ($p < 0.05$) and age ($p < 0.001$), while turquoise module was significantly positively correlated with age ($p < 0.001$) (Figure 3A). In summary, we observed age and genotype-by-diet effects on the lightyellow module, while the turquoise module is driven primarily by age and not diet. We also observed that the diet and age driven lightyellow module was significantly correlated ($p < 0.05$) with multiple assays such as NfL, frailty score, plasma cytokines (interleukin [IL]1β, IL10, IL5, IL6, KC-GRO) (Figure 3B, Figure S4). In contrast, the age driven turquoise module was significantly correlated ($p < 0.05$) with effect of age on behavior and weakly correlated with a few plasma cytokines (IL2, interferon gamma [IFN-γ]) and inflammatory cell counts (Iba1 and GFAP counts) (Figure 3B, Figure S4). The lightyellow module was uniquely driven by both age and diet and demonstrated strong positive associations with AD biomarkers such as NfL and multiple cytokines.

We further assessed the enrichment of AD biological domains[14] in gene modules. We found that genes in lightyellow modules were significant enriched for the Apoptosis (odds ratio = 1.90, $p = 2.11 \times 10^{-4}$), Immune Response (odds ratio = 1.63, $p = 3.67 \times 10^{-3}$), Lipid Metabolism (odds ratio = 2.01, $p = 3.64 \times 10^{-6}$), Oxidative Stress (odds ratio = 1.76, $p = 3.32 \times 10^{-2}$), and Vasculature (odds ratio = 2.14, $p = 1.14 \times 10^{-4}$) AD biological domains (Figure 3C–D; Table SB3). We also identified GO-terms associated with these biological domains that are significantly enriched in lightyellow gene modules (Figure 3C–D, Table SB3). On the other hand, genes in the turquoise module were prominently enriched for the Immune Response biological domain (odds ratio = 2.39, $p = 1.8 \times 10^{-49}$) (Table SB3). These data suggest that age is the strongest risk factor for driving inflammatory changes,

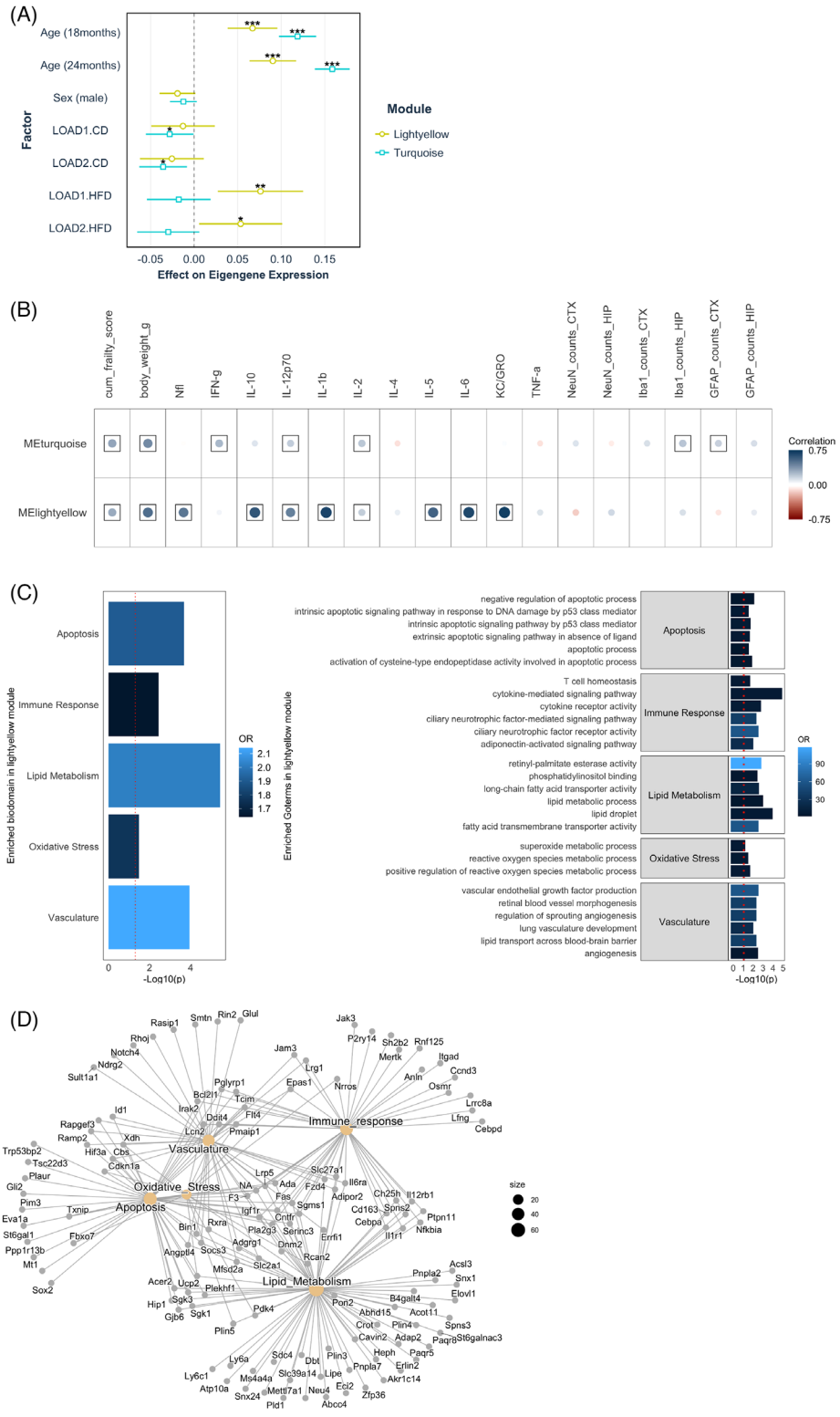

FIGURE 3 A gene module associated with AD biomarkers is driven by age and high-fat/high-sugar diet. The lightyellow gene module was associated with advanced age ($p < 0.001$) and both genotypes on HFD ($p < 0.05$), while the turquoise module was primarily associated with age ($p < 0.001$) (A). Correlations between the turquoise and lightyellow module eigengenes. Lightyellow was significantly correlated with frailty score, body weight, NfL, and many plasma cytokines (IL-1β, IL-2, IL-12p70, IL-10, IL-5, IL-6, KC-GRO), while the age-driven turquoise module was correlated with behavioral assay (frailty score and body weights) and weakly correlated with a few plasma cytokines (IL-2, IFNγ) and inflammatory cell counts (IBA1 and GFAP counts) (B). Positive correlation coefficients are shown in blue and negative correlations in red, proportional to color intensity and circle size, with frames for significant correlations (FDR < 0.05). AD-related biological domain enrichment analysis in the age and HFD driven lightyellow module gene set using Fisher exact test, with the top six enriched GO terms within each enriched bidomain (C). Network of genes in each enriched biological domain and the lightyellow module (D). AD, Alzheimer's disease; HFD, high-fat diet.

while diet effects in aged LOAD mice are associated with multiple AD endophenotypes such as lipid metabolism, immune response, and oxidative stress.

3.3 | Aging × LOAD genetic risk × environment reveals proteomic changes characteristic of AD

Tandem mass tag proteomics were performed on hemibrains from LOAD1 and LOAD2 mice at 4, 12, and 18 months of age on control diet. LOAD1 and LOAD2 mice fed HFD were also assayed at 18 months, paired with B6J controls on CD. A total of 10,406 proteins were quantified across 106 samples. To focus on effects in aged mice, we assessed protein expression changes in 18 month old LOAD1 and LOAD2 mice on CD and HFD compared to age-matched B6J mice on CD by one-way analysis of variance (ANOVA) with post-hoc Tukey significance testing (Table SC). In LOAD1 mice on CD, we observed 1666 significantly differentially expressed proteins (838 upregulated, 828 downregulated) (padj < 0.05), while a total of 2590 proteins were significantly differentially expressed (1237 upregulated, 1353 downregulated) (padj < 0.05) in LOAD1+HFD compared to B6J mice on CD (Table SC). In LOAD2+CD, we observed a total of 1102 significantly differentially expressed proteins (535 upregulated, 567 downregulated) (padj < 0.05) while in LOAD2+HFD we observed 1839 significantly differentially expressed proteins (897 upregulated, 942 downregulated) (padj < 0.05). We therefore observed hundreds of differentially expressed proteins in both LOAD1 and LOAD2, with greater numbers for both strains on HFD.

To assess disease-relevant aspects of mouse models, we performed a correlation analysis between mouse models and 44 human proteomics modules from a LOAD study of the dorsolateral prefrontal cortex.[15] These modules were functionally annotated and named based on protein enrichments and each was assessed for eigenprotein correlations to AD traits including neuropathological markers and cognitive outcomes.[15] Twelve modules were significantly correlated to one or more traits, referred to here as AD modules.[15] We compared protein expression changes in LOAD1 and LOAD2 mice relative to B6J mice at 18 months with changes observed in human AD subjects versus controls for each human protein module. This procedure allowed module-wide assessment of coordinated protein changes and therefore determined murine reproduction of each module that characterizes human LOAD.

LOAD1 and LOAD2 mice were significantly and positively correlated ($p < 0.05$) with multiple common human AD modules. These included M1_Synapse_Neuron, M3_Oligo_Myelination, and M12_Cytoskeleton (Figure 4A; Table SD). The M2_Mitochondria module exhibited significant positive correlation ($p < 0.05$) with all mouse models except LOAD2 mice on HFD, for which a positive correlation did not reach significance ($p = 0.06$) (Figure 4A; Table SD). Additional correlations reaching significance included LOAD1 mice on HFD and LOAD2 mice on both diets with M22_Post-Synaptic_Density and M38_Heat_Shock_Folding modules (Figure 4A; Table SD). LOAD2+HFD additionally showed significant positive correlations with M4_Synapse_Neuron, M7_MAPK_Metabolism, and M43_Ribonucleoprotein_Binding modules (Figure 4A; Table SD), whereas other mice (LOAD1+CD, LOAD1+HFD and LOAD2+CD) were positively correlated but below the significance threshold.

Overall, we detected genetic effects from aged LOAD1 and LOAD2 mice that correlated with multiple human AD proteomics modules that were generally enhanced by exposure to HFD, especially in LOAD2 mice. LOAD2+HFD were positively correlated with 10 of the 44 total protein modules, of which 5 modules (M1_Synapse_Neuron, M3_Oligo_Myelination, M4_Synapse_Neuron, M7_MAPK_Metabolism, and M22_Post-Synaptic_Density) were correlated with AD traits.[15] These modules frequently represented neuronal proteins, distinct from the immune and metabolic signatures observed in transcriptomic analyses.

To better understand the functions of proteins driving the significant positive correlations between LOAD2 mice on HFD and human AD, we isolated the proteins within each module with common directional changes (increased or decreased abundance) for LOAD2+HFD and human AD cases. We performed gene ontology enrichment analysis on these proteins. Proteins that showed mouse-human directional coherence in the M1_Synapse_Neuron module were enriched for biological functions including "synaptic vesicle cycle," "vesicle-mediated transport in synapse," and "synapse organization" (Figure 4B; Table SE). Proteins that showed directional coherence in the M4_Synapse_Neuron module were enriched for "synaptic vesicle cycle" and "exocytosis" biological functions (Figure 4B; Table SE). In the M22_Post-Synaptic_Density module, coherent mouse-human proteins were enriched for biological functions including "synapse organization," "postsynapse organization," and "dendrite development" (Figure 4B; Table SE). These functions represent the core neuronal processes recapitulated in LOAD2+HFD at the protein level.

Proteins in these synaptic AD protein modules mostly had reduced abundance in LOAD2.HFD mice (logFC < 0) compared to chow-fed B6J controls. This reduced expression of proteins associated with synapse/neuronal functions was similar to human AD cases (Figure 4C), although we note these mice did not exhibit frank neurodegeneration.

For non-synaptic modules, we found coherent proteins in the M3_Oligo_Myelination module were enriched for biological functions including "oligodendrocyte differentiation," "myelination," and "microtubule organization" (Figure 4B; Table SE). Proteins with directional coherence in the M7_MAPK_Metabolism module were enriched for biological functions such as "regulation of transforming growth factor beta production" and "carbohydrate metabolic process" (Figure 4B; Table SE). In the M28_Ribosome_Translation module, protein abundances mostly increased (logFC > 0) and were enriched for "ribosome biogenesis" and "cytoplasmic translation" (Figure 4B–C; Table SE). Finally, coherent proteins in the M38_Heat_Shock_Folding module were enriched for "protein folding" and "chaperone-mediated protein folding" biological functions (Figure 4B; Table SE). Proteins exhibiting directional coherence in the M3_Oligo_Myelination and M7_MAPK_Metabolism modules generally had greater abundances in LOAD2+HFD mice compared to B6J controls and human AD cases, corresponding to increased protein expression associated with "MAPK_metabolism" and "Oligo myelination" (Figure 4C).

FIGURE 4 LOAD mice exhibit proteomics changes similar to human LOAD. Correlation coefficients between 18-month-old LOAD mouse models and 44 human proteomics co-expression modules [Johnson et al Ravi's ref [9]] (A). Modules in bold face were significantly correlated to one or more AD traits. Circles correspond to positive (blue) and negative (red) Pearson correlation coefficients for protein expression changes in LOAD mice (log fold change of LOAD strains vs. B6J) and human disease (log fold change for cases vs. controls). Color intensity and size of the circles are proportional to the Pearson correlation coefficient, with significant correlations ($p < 0.05$) framed. Five top enriched GO terms for proteins with common directional changes for 18-month-old LOAD2 mice on HFD and human AD cases (B). Protein module network with common directional changes for 18-month-old LOAD2 mice on HFD and human proteomics modules (C). Blue (red) nodes correspond to increased (reduced) protein abundance in both 18-month-old LOAD2 HFD mice compared to B6J mice and human AD cases versus controls. AD, Alzheimer's disease; HFD, high-fat diet.

3.4 | Aging × LOAD genetic risk × environmental risk reveals age-dependent changes in brain volume

Longitudinal volumetric measurements were employed to elucidate age-dependent alterations in brain volume within Cohort 2. Building upon the findings derived from Cohort 1 at JAX, which encompassed indicators such as neuronal cell loss, increased levels of neurofilament light chain (NfL), and molecular manifestations of neuronal cell dysfunction (refer to Figures 1–4), Cohort 2 was established at Indiana University. This cohort consisted of male and female mice designated as LOAD1 and LOAD2, subjected to either a standard control diet (CD) or a high-fat diet (HFD). The primary objective at Indiana University was to assess brain volumes through in vivo magnetic resonance (MR) imaging and to conduct a comprehensive evaluation of LOAD2+HFD mice for plasma and brain biomarkers, with potential implications for preclinical testing.

In vivo MR imaging was conducted on LOAD2 CD and HFD-fed mice at 4, 12, and 18 months of age. The mean whole brain volumes for male LOAD2 CD and HFD mice were 478.56 ± 18.63 and 459.56 ± 6.41 mm^3 at 4 months, 464.53 ± 15.16 and 468.40 ± 9.83 mm^3 at 12 months, and 502.68 ± 13.59 and 470.25 ± 6.37 mm^3 at 18 months, respectively. Correspondingly, the mean whole brain volumes for female LOAD2 CD and HFD mice were 468.19 ± 7.28 and 467.42 ± 6.52 mm^3 at 4 months, 479.84 ± 12.60 and 483.48 ± 8.20 mm^3 at 12 months, and 507.29 ± 11.46 mm^3 and 487.37 ± 11.86 mm^3 at 18 months.

Statistical analysis revealed a significant reduction in brain volume was observed at 4 and 18 months in LOAD2+HFD male mice (4 months, $p = 0.0225$ and 18 months, $p = 7.88e\text{-}6$; Table SF), while no significant difference was observed at 12 months ($p = 0.5134$; Table SF). For LOAD2 female mice on a HFD, a significant difference was observed at 18 months ($p = 0.0186$), but no significant disparities at 4 months ($p = 0.812$; Table SF) or 12 months ($p = 0.4911$; Table SF).

Among the 165 brain labels analyzed, 45, 57, and 95 brain areas exhibited significant volumetric reductions at 4, 12, and 18 months, respectively, for male mice. Similarly, for female mice, 47, 67, and 51 brain areas displayed significant reductions at 4, 12, and 18 months. Volumetric statistical maps were generated for both male and female LOAD2 CD and HFD mice at the time points, and the significant areas were superimposed onto the T2-weighted template image. Notably, the analyses unveiled a progressive increase in the

number of significant areas with advancing age of the mice (Figure 5A,B; Table SF).

3.5 | Aging × LOAD genetic risk × environment exacerbates inflammation

We next used cohort 2 mice to identify cytokines in the plasma and brain that may be utilized as biomarkers for preclinical testing. Analysis of NfL and cytokines in the plasma revealed an increase in NfL at 12 months in HFD males (Figure 5C). By 18 months, however, the HFD effect was absent, but an increase in NfL was driven by age (Figure 5C). Aβ40 was lower in males fed a HFD at 12 and 18 months, but the same difference was not observed in females; Aβ42 levels were not significant at any time point, likely due to variability among groups, however, there was an overall trend for a reduction in Aβ42 in males fed a HFD at 12 and 18 months (Figure 5D,E). In HFD animals, we found significant increases in TNFα in LOAD2+HFD males at 12 and 18 months, females were approaching a significant increase by 18 months, but did not reach significance (Figure 5F). Additional proinflammatory cytokines were examined (Figure 5G–J), with reductions in IFNγ observed in HFD males at 12 and 18 months and age-related alteration in IL-6, IL-2 and IL1β. Interestingly, as a confirmation and extension of these data and to demonstrate cross-laboratory replicability, we also observed sustained TNFα levels in HFD mice from Cohorts 4 and 5 (University of Pittsburgh). LOAD2+HFD males from 2 months of age in Cohort 4 maintained significantly higher concentrations of TNFα in their plasma from 7 months of age onward compared to LOAD2 males fed CD, while females on HFD appeared to follow a similar trend as males but only reached significance at 8–8.5 and 15–18 months of age.

At 18 months of age, the brains from longitudinal cohort 2 were processed for biochemistry and neurodegeneration. In the brain, female LOAD2+HFD had increased insoluble Ab42 (Figure 6A), but both males and females on a HFD had reduced insoluble Ab40 and soluble Ab40 and 42 (Figure 6B–D). With regard to proinflammatory cytokines, HFD reduced IL-5 and IL-4 in females (Figure 6F–G), but increased IL-2, KC-GRO, and IL-12 in both males and females (Figure 6H–J). Interestingly, in the brain (as compared to plasma), TNFa (Figure 6K) remained unchanged. Anti-inflammatory IL-10 was increased in males and females on a HFD (Figure 6L). Similar to cohort 1, neurodegeneration and gliosis were also measured in the cortex and subiculum (Figure S5). At 18 months old, GFAP and IBA1 were increased in female mice on a high-fat diet in the cortex.

3.6 | Aging × LOAD genetic risk × environmental risk alters neurovascular phenotypes

Cohort 3 mice (female and male LOAD1 and LOAD2 mice on CD and HFD) were established at Indiana University (see the Methods section and Companion Article in this Issue) to assess neurovascular uncoupling of ^{18}F-FDG and ^{64}Cu-PTSM, as measurements of cerebral glucose uptake and brain perfusion. Consistent with transcriptomics (Figure 3—4), along with blood and brain cytokines (Figures 5—6), the addition of HFD to 12-month LOAD1 mice (relative to 12-month LOAD on CD) resulted in a Type 1 neurovascular uncoupling (i.e., reduction cerebral glucose uptake and an increase brain perfusion) of perfusion and glycolytic metabolism, which was sexually dimorphic in nature. Across multiple brain regions, denoted by region annotation (Figure 7A), female LOAD1 mice showed a significant reduction in glucose uptake, coupled with an elevation in perfusion of the same brain regions relative to 4 month cohorts, consistent with a cytokine-driven diabetic phenotype. Statistical comparison revealed that dorsal-medial-ventral areas of the Auditory Cortex (AuDMV), Dysgranular Insular Cortex (DI), Lateral Orbital Cortex (LO), Primary Motor (M1) and Secondary Motor (M2) Cortex, Parietal Association Cortex (PtA), Retrosplenial Dysgranular Cortex (RSC), Primary Somatosenory Cortex (S1), and Thalmus (TH) were significantly different ($p < 0.05$, unpaired two-tailed *t*-test) relative to the control diet groups in female mice (Figure 7A, top panel). By comparison, regional uncoupling analysis of male LOAD1+HFD only showed significant changes ($p < 0.05$, unpaired two-tailed *t*-test) in the Dorsolateral Orbital Cortex (DLO), Primary Motor (M1), and Secondary Motor (M2) Cortices.

Importantly, the addition of hAβ onto the LOAD1 background (yielding LOAD2), showed a Type 2 neurovascular uncoupling (i.e., increased cerebral glucose uptake and a reduced brain perfusion) phenotype when placed on a HFD (relative to LOAD2 on a CD), which was only observed in the female cohort. Unlike LOAD1 mice, female LOAD2 mice on a HFD showed a significant increase in glucose uptake concomitant with regional reductions in tissue perfusion (Figure 7B) and aligned with the transcriptomic network changes (Figure 3B), and blood cytokine levels for TNFα, IL1β, and IL6 (Figure 5). Statistical analysis of brain regions revealed that Corpus Callosum (CC), Entorhinal Cortex (ECT), LO, Medial Orbital Cortex (MO), Perirhinal Cortex (PRH), Prelimbic Cortex (PRL), and Ventral Orbital Cortex (VO) all were significantly different ($p < 0.05$, unpaired *t*-test) from control diet groups (Figure 7A, top panel) in female LOAD2 mice. By contrast, male LOAD2+HFD showed different brain regions, which were uncoupled with treatment, with the AuDMV, Dorsintermed Entorhinal Cortex (DLIVEnt), ECT, PRH, RSC, Temporal Association Cortex (TeA), and Primary and Secondary Visual Cortex (V1V2).

To elucidate the role of aging on gene × environmental effect, we performed neurovascular uncoupling analysis on LOAD2 mice at 18 months. Unlike LOAD1 and LOAD2 at 12 months which showed a Type 1 and Type 2 uncoupling phenotype respectively, LOAD2 at 18 months revealed a hypermetabolic and hyperperfused phenotype in both sexes, which resulted in nearly all brain regions increasing in glucose uptake paired with increases in tissue perfusion (Figure 7C). This increase in both perfusion and metabolism at this age is consistent with the plasma cytokine data (Figure 8) that show a significant elevation in TNFα, IL-6 and IL-5, which are markers of cell activation and proliferation and are consistent with clinical reports of prodromal conversion from healthy controls to MCI.

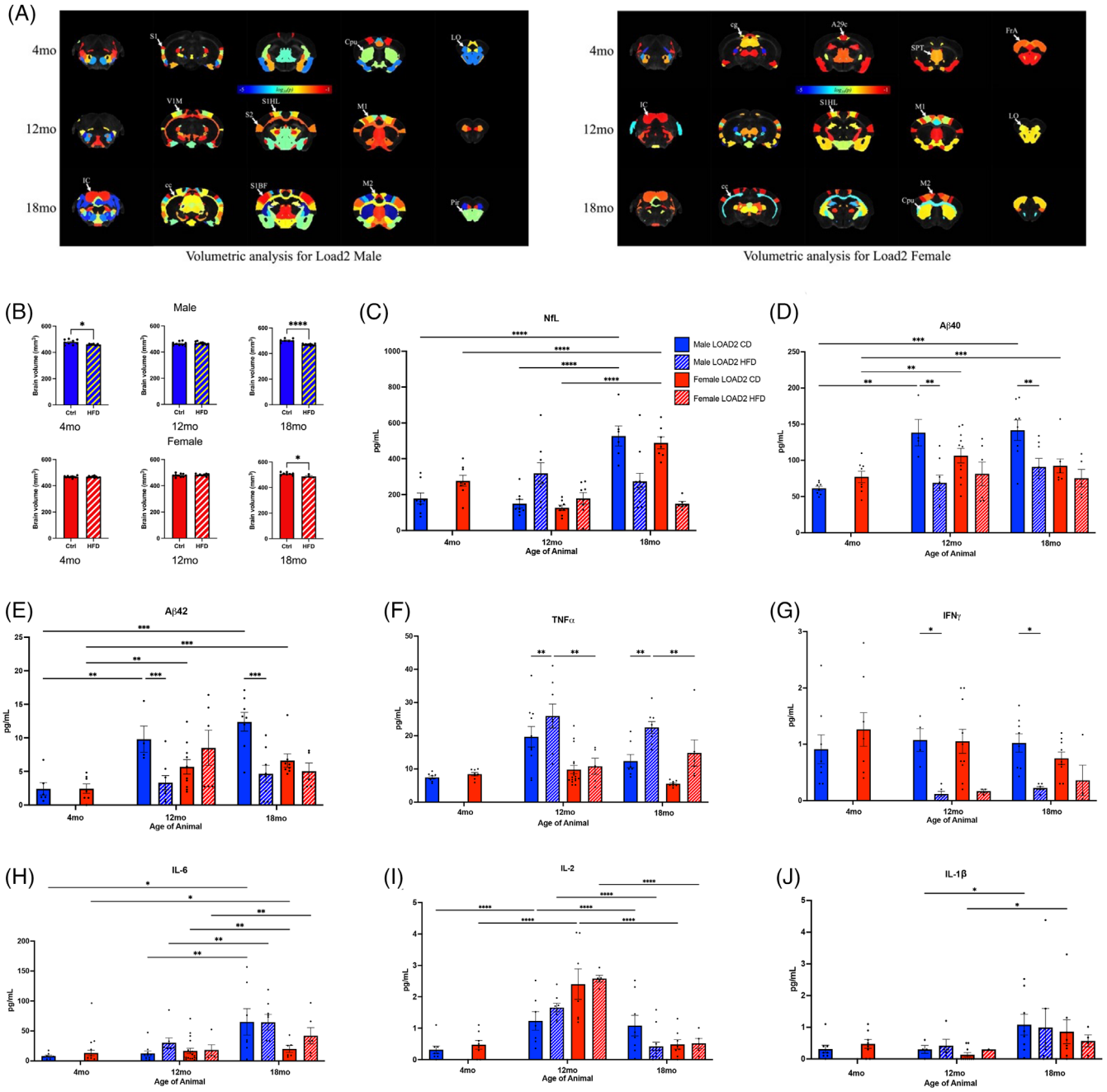

FIGURE 5 High-fat diet reduces brain volume in multiple brain regions and alters plasma biomarkers. Volume statistics map for LOAD2 males at 4, 12, and 18 months. The significant brain areas were overlaid over gray scale subject template image. (The *p*-values were converted into logarithmic scale between range −5 and −1. Volume statistics maps for Load2 female at 4, 12, and 18 months. The significant brain areas were overlaid over gray scale subject template image. The p-values were converted into logarithmic scale between range −5 and −1.) (A). Bar plot showing whole brain volume for CD and HFD groups for male and female cohorts at age groups 4, 12, and 18 months, respectively (B). Longitudinal assessment of peripheral plasma from male and female LOAD2 animals provided CD or HFD measured levels of NfL (C) and Aβ species (40 and 42; panels D and E, respectively). Cytokines related to inflammation regulation were also measured and include TNF-α (F), IFNγ (G), IL-6 (H), IL-2 (I), and IL-1β (J). Two-way ANOVA $^{*}p < 0.05$, $^{**}p < 0.01$, $^{***}p < 0.001$, $^{****}p < 0.0001$. A29c, cingulate cortex; cc, corpus callosum; cg, Cingulum; Cpu, striatum; FrA, frontal association area; IC, inferior colliculus; LO, lateral orbital cortex; M1, primary motor cortex; M2 secondary motor cortex; Pir, piriform cortex; S1BF Primary Somatosensory Cortex, Barrel Field; S1HL Primary Somatosensory Cortex, Hindlimb; S1, Primary Somatosensory Cortex; SPT, Septum; S2, Secondary Somatosensory Cortex; V1M, Primary Visual Cortex, Monocular area.

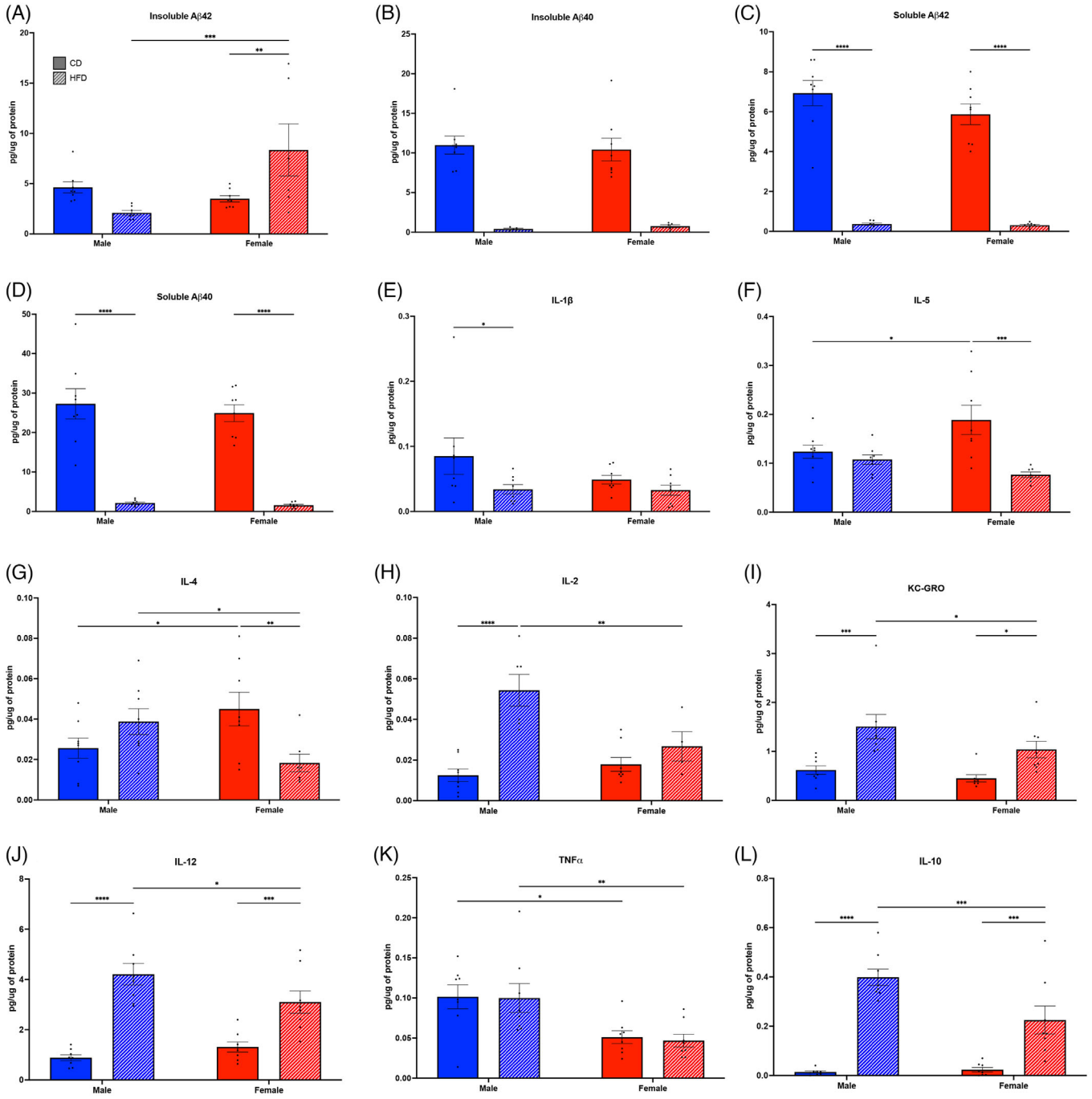

FIGURE 6 Brain biomarkers in a longitudinal cohort of LOAD2 mice fed a high-fat diet. Whole brain lysates from 18-month-old animals were analyzed by ELISA for biomarkers and cytokines aligned with inflammation and disease progression. For changes related to sex, genotype, and diet measurements are provided for insoluble Aβ42 (A) and Aβ40 (B); soluble Aβ42 (C) and Aβ40 (D); IL-1β (E); IL-5 (F); IL-4 (G); IL-2 (H); KC-GRO (I); IL-12 (J); TNF-α (K); and IL-10 (L). Analysis by two-way ANOVA $^{*}p < 0.05$, $^{**}p < 0.01$, $^{***}p < 0.001$, $^{****}p < 0.0001$.

3.7 | Disease trajectory from adolescence through aging × LOAD genetic risk × environmental risk

To further consider the relevance of the LOAD2 mice as a model for preclinical testing, a group of male and female LOAD2 mice fed a CD or HFD from 2 months of age (cohort 4) and a group of male and female LOAD2 and WT littermate controls fed CD or HFD from 6+ months of age (cohort 5) were established at the University of Pittsburgh. The goal of these cohorts was to track longitudinal biomarker measures for cytokines and Aβ throughout aging, in order to investigate the inflection point at which biomarkers revealed pathological consequences of environment × aging × gene effects, in order to identify a window for therapeutic intervention for future preclinical testing. In addition to biomarker analysis through aging, the cohort were also evaluated for cognitive function assessed by a touchscreen testing battery as well as evaluating the effects of food restriction necessary for

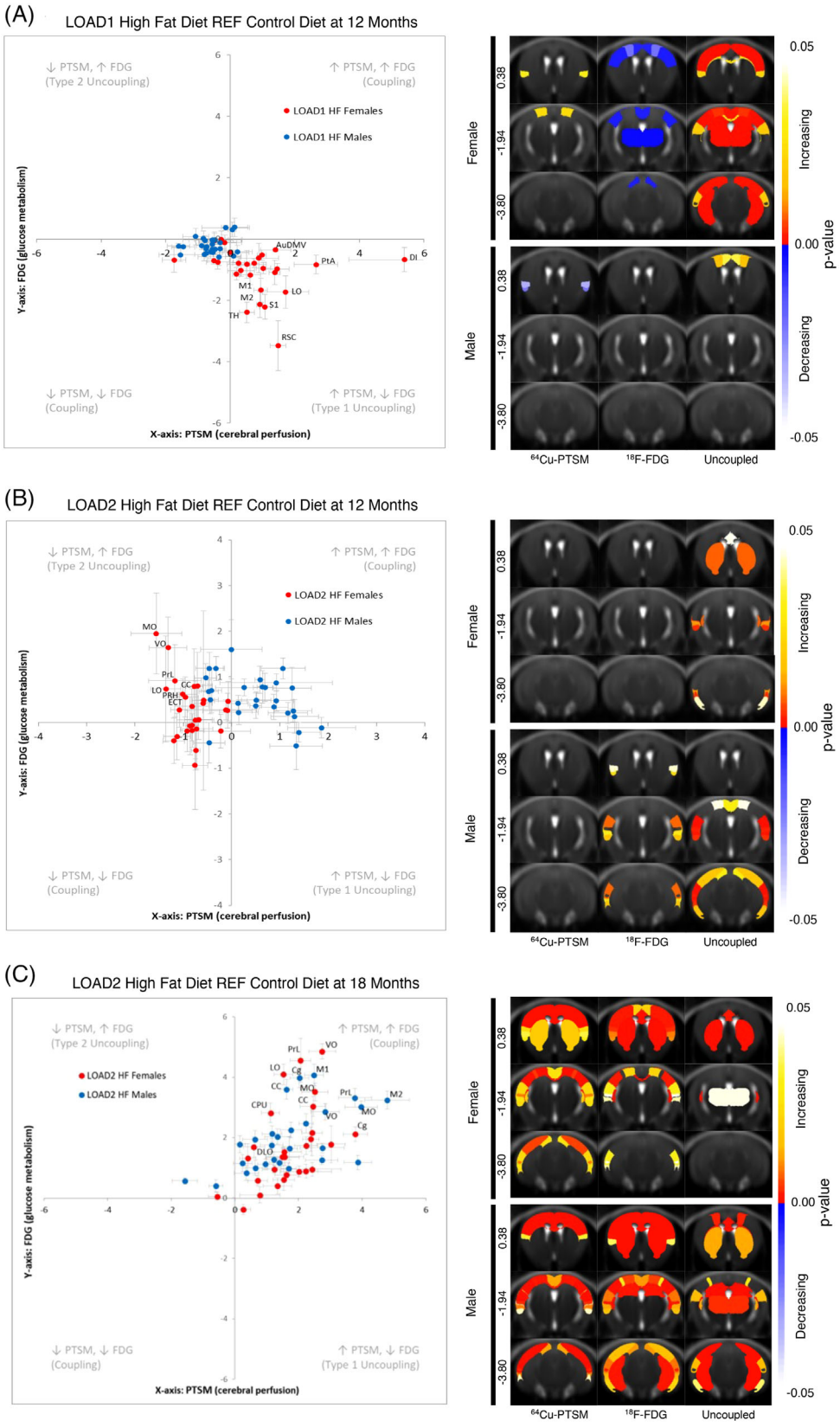

FIGURE 7 Neurovascular Uncoupling of LOAD1 and LOAD2 mouse models. The degree of neurovascular coordination in LOAD1 (A) and LOAD2 mouse models (B) conditioned on high-fat diet (HFD), we performed uncoupling analysis. (Left) Uncoupling analysis chart in male (blue) and female (red) mice at 12 months, with many brain regions showing significant decreases in metabolism with increases in perfusion. LOAD2 animals aged to 18 months (C) were similarly analyzed. (Upper Right) Female and (Lower Right) Male *p*-value males showing which regions were significantly different for perfusion, metabolism, and uncoupling. HFD, high-fat diet.

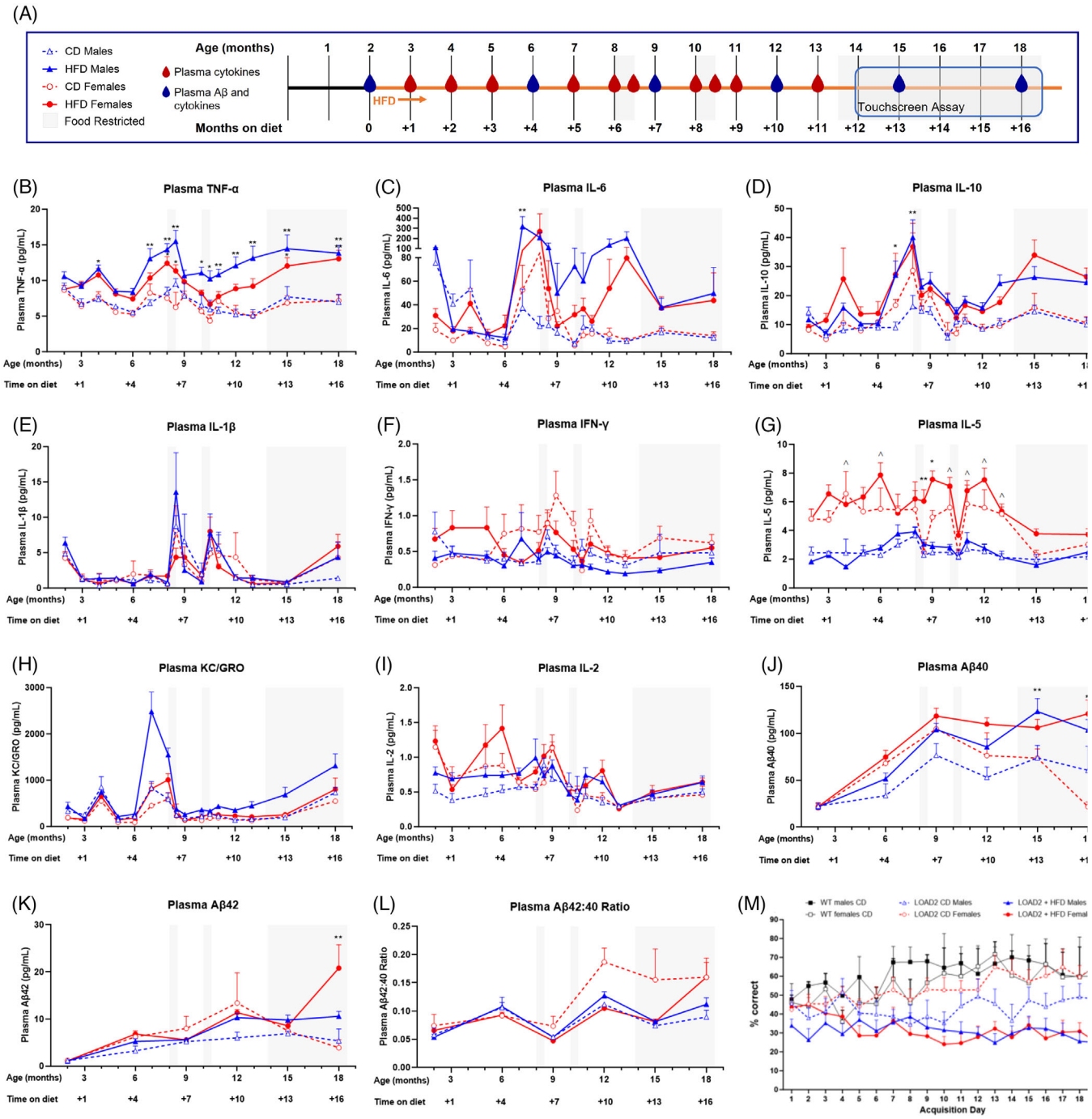

FIGURE 8 Comprehensive validation of LOAD2 mouse model for preclinical drug testing. As a confirmation and extension of initial characterization data of the LOAD2 mouse model conditioned on high-fat diet (HFD) to serve as a potential model for preclinical testing, independent cohorts were evaluated for disease trajectory of serial plasma biomarkers and cognitive testing. (A) Illustration of timeline and procedures; (B) plasma TNF-α (pg/mL); (C) plasma IL-6 (pg/mL); (D) plasma IL-10 (pg/mL); (E) plasma IL-1β (pg/mL); (F) plasma IFNy (pg/mL), (G) plasma IL-5 (pg/mL); (H) plasma KC-GRO (pg/mL); (I) plasma IL-2 (pg/mL); (J) plasma Aβ40 (pg/mL); (K) plasma Aβ42 (pg/mL); (L) calculated Aβ 42:40 ratio in plasma; (M) learning curves of aged (14+ month) LOAD2 mice $\pm$ HFD in comparison to age- and sex-matched WT controls during the acquisition phase of the touchscreen cognitive testing battery. Plasma cytokines and plasma Aβ were measured using MesoScale Discovery multiplex ELISA kits in accordance with the manufacturer's protocol. HFD, high-fat diet.

touchscreen testing and its impact on cytokine levels (Figure 8 and Figure S6).

Similar to cohort 2 at IU (Figure 5F), LOAD2 males fed HFD in cohort 4 had increased levels of plasma TNFα at 12 and 18 months of age relative to LOAD2 males fed CD (12 months, $p = 0.0001$; 18 months, $p = 0.0002$). In fact, analysis of monthly plasma cytokines revealed increased TNFα as early as 4 months of age ($p = 0.0377$) with consistent increases from 7 months of age onward in LOAD2+HFD males compared to LOAD2+CD males ($p < 0.05$, Figure 8B). The effects of HFD on plasma TNFα was less robust in females, consistent with data from cohort 2 at IU. We observed an overall trend of higher concentrations of plasma TNFα in females fed HFD compared to females fed CD, but those levels were significantly different only at 8–8.5 months ($p < 0.05$) and 15–18 months of age ($p = 0.0198$ at 15 months and $p = 0.0068$ at 18 months; Figure 8A). In addition to TNFα, we also measured nine other cytokines, seven of which were above the lower limits of detection (see Supplemental methods). Plasma levels of IL-6 ($p = 0.0022$) and IL-10 ($p = 0.0375$) were significantly higher in LOAD2+HFD males compared to LOAD2+CD males at 7 months of age, and levels of IL-10 ($p = 0.0025$) but not IL-6 ($p = 0.0832$) were also higher at 8 months of age in HFD males (Figure 8C,D) prior to the first trial of food restriction that preceded touchscreen testing. Interestingly, plasma levels of IL-5 were significantly higher in LOAD2 females, regardless of diet, compared to males at several time points ($p < 0.05$, Figure 8G) while other plasma cytokines measured—IL-1β, IFNγ, KC-GRO, and IL-2 (Figures 8E,F,H, and I)—did not show diet- or sex-related effects in this cohort. In cohort 5, the middle-aged (6–12 months old) start for HFD (Figure S6A) produced a more modest effect on plasma TNFα with LOAD2+HFD males showing higher concentrations of plasma TNFα at 4 months on diet relative to WT males on CD ($p = 0.0241$) and at 5 months on diet relative to LOAD2 and WT males on CD ($p = 0.0451$ and $p = 0.0034$), LOAD2+HFD females showing higher concentrations of TNFα relative to LOAD2+CD females only at 5 months on diet ($p = 0.0291$), and WT males but not females on HFD showing higher concentrations of TNFα relative to WT+CD mice also only at 5 months on diet ($p = 0.0091$ males and $p = 0.998$ females, Figure S6B). In all other cytokines measured—IL-6, IL-10, IL-1β, IFNγ, IL-5, KC-GRO and IL-2 (Figure S6C–I)—there was no significant effect of diet on LOAD2 or WT males or females, though we did again observe a sex-effect in plasma IL-5 with concentrations being higher in LOAD2 females compared to LOAD2 males regardless of diet ($p < 0.01$ at 2 months on diet and $p < 0.05$ at 3 months on diet, Figure S6G).

Concentrations of plasma Aβ40 and 42 were also altered by HFD in cohort 4 (Figure 8J–K) and by genotype but not diet or sex in cohort 5 (Figure S6J,K) consistent with the observation that HFD started earlier in life (cohort 4) produces a more robust phenotype than when initiated midlife (cohort 5). Analysis of WT and LOAD2 mice exposed to HFD at middle-age (6+ months age) revealed a less aggressive phenotype as indicated by lower plasma cytokine levels and lower plasma Aβ40 and Aβ42 when compared with plasma levels from mice exposed to HFD at 2 months of age (Figure 8). Male LOAD2 mice +HFD beginning from 2 months of age had increased levels of plasma Aβ40 at 15 ($p = 0.01$) and 18 months of age ($p = 0.0365$) relative to LOAD2+CD males while female LOAD2+HFD beginning from 2 months of age had increased plasma Aβ40 at 18 months ($p < 0.0001$) relative to LOAD2+CD females (Figure 8J). As demonstrated in Figure S7A LOAD2 mice beginning HFD at 6+ months of age (cohort 5) failed to demonstrate increases in plasma Aβ40 relative to LOAD2+CD (Figure S6J). Plasma Aβ42 was significantly increased in LOAD2+HFD females from cohort 4 compared to LOAD2+CD females at 18 months of age ($p < 0.0001$, Figure 8K) and compared to age-matched WT+CD females ($p = 0.0319$, Figure S6K).

We assessed the cognitive function of both cohorts 4 and 5 using a touchscreen assay battery. Touchscreen tasks were specifically selected as they evaluate subjects in daily tasks for an extended timeframe of several months and are sensitive to detecting more mild cognitive changes across cognitive domains relative to acute assays that require only minutes of behavioral evaluations. More specifically, by evaluating daily accuracy levels through acquisition of different tasks, the sensitivity and resolution of the assay can provide insight to attenuated or milder phenotypes as opposed to typical binary measures of cognitive function.

During the initial associative learning, pretraining phase of the task in which subjects were required to demonstrate the ability to pair the presentation and touch response to the visual stimuli with the presentation of the reward, all subjects irrespective of age, genotype, diet, or sex, demonstrated intact associative learning and completed the pretraining steps (Figure S7). Within control diet groups, there was no effect of genotype or sex ($p > 0.05$ for WT+CD vs. LOAD2+CD). Interestingly, LOAD2+HFD mice required a greater number of days to meet criteria relative to LOAD2 mice on control diet [one-way ANOVA [$F(3, 24) = 5.290$; $p = 0.0061$; Figure 8M] despite similar food restriction. Within sex analysis revealed a statistically significant increase in females reared on HFD (*T*-test; $p < 0.05$) and a modest non-significant increase in males reared on HFD (*T*-test; $p = 0.38$). These data indicate that associative learning was intact across all genotypes and treatment (CD v HFD) in these aged mice in the absence or presence of genetic (LOAD) and environmental (HFD) risk.

During the acquisition phase of the location discrimination task in which measures of accuracy are of the primary measure to determine learning, 100% of both LOAD2+CD and WT+CD mice met advancement criteria with accuracy levels to a priori criterion of ≥70%; while subjects exposed to HFD failed to meet this criteria (Figure 8) This advancement criteria is significantly greater than chance levels in this assay and was selected to accommodate performance in advanced aged mice for the present studies as previous data comparing young versus aged mice on touchscreen tasks shows that aged mice have impaired accuracy relative to young mice; thus >70% is acceptable and greater than chance for completing this task (see ref. [16]). Analysis of accuracy levels during initial acquisition of the task (Training Days 1–18) revealed a statistically significant impairment in HFD treated subjects relative to genotype and age- and sex-matched non-HFD controls as measured by two-way repeated measures ANOVA: [$F(5, 33) = 9.047$; $p < 0.001$; Figure 8M]. The lack of ability to learn the task in HFD mice is unlikely to be explained by food motivation, as both HFD and CD groups were sufficiently restricted, and all groups

independent of diet or genotype acquired the initial touch-reward association (Figure S6). It is important to note that the present studies used a 10% sucrose solution for the reward which is a departure from the standard touchscreen protocols that use strawberry flavored milkshake-based rewards.[17] We intentionally chose to avoid milk-based rewards given that the constituents of milk and dairy products may contribute to attenuation of AD related pathologies including amyloid deposition and inflammation.[18–20] Notably 10% sucrose is a common and well-established reinforcer for mice in operant based tasks and therefore was a salient alternative as evidenced by the ability of all subjects to demonstrate consumption of the reward and acquire the touch-reward association during the initial phase of the task. This indicates that the failure of HFD mice to accurately perform the task is more likely a feature of impaired learning due to the combination of advanced age × environmental risk (e.g., HFD), than reward salience. Further studies may be required to investigate methods for enhancing motivation for rewards in mice reared on HFD which may include more aggressive water restriction protocols as HFD treated mice even in the presence of strawberry-milk shake reinforcer also have issues with touchscreen tasks (personal communication with Dr. Lisa Saksida, also see ref. [21]). Figure S6M illustrates performance of aged (18+ month) LOAD2 mice on CD (purple diamonds) and age- and sex-matched C57BL/6J (WT) mice on control diet (n = 3–5 per genotype) on the LD task for both large (easy) and small (hard) separation conditions (mean ± s.e.m.). As expected, the increase in task difficulty was significant across genotypes as measured by increased number of trials required to reach criterion for easy relative to hard [$F(1, 12) = 5.156$; $p = 0.04$]. While there was a modest increase in the number of trials to reach criterion in LOAD2 mice relative to WT the effect of genotype was not significant [$F(1, 12) = 0.4134$; $p = 0.53$].

4 | DISCUSSION

Despite the recent approval of anti-amyloid therapies, improved therapies for LOAD are needed. One key to this is the development of preclinical models that more faithfully recapitulate the complexity of LOAD. Here we introduce LOAD2 that, although lacks hallmark amyloid and tau pathologies, in combination with a HFD, shows age- and sex-dependent development of key aspects of LOAD. At 18 months of age, female LOAD2+HFD, but not controls (e.g., LOAD2 fed a CD or LOAD1 mice fed a HFD) show small but significant loss of cortical neurons. The mechanisms of neuronal cell loss and, given specific circuits are differentially susceptible to aging and/or AD,[22–25] whether neuronal cell loss is as a result of sporadic loss of neurons or loss of neurons within specific circuity are still to be determined. We also observed increased levels of insoluble Aβ42, brain region-specific volumetric changes, neurovascular uncoupling, and cognitive deficits, consistent with prodromal stages of AD. These changes correlated with a clinically relevant elevation in plasma NfL—and combined emphasize the robustness of modeling genetics × age × environment.

As observed in human AD,[15] we detected distinct proteomic and transcriptomic signatures in our LOAD mouse models. Transcriptomic signals tended to represent immune, vascular, and lipid metabolism (Figure 3), whereas proteomic signatures were focused in synaptic and myelination modules (Figure 4). The advent of proteomic technologies that commonly quantify around 10,000 proteins, such as the TMT approach used here, now enable deep characterization to reveal such differences. We also note that the AD-relevant transcriptomic changes tended to be driven by age and diet (Figure 3A) while the proteomic changes were primarily due to APOE4 and *Trem2*R47H* genetics and somewhat exacerbated by diet. These results demonstrate the importance of multi-omic analyses in fully characterizing causal factors (e.g., genetics, diet, age) and affected processes (e.g., synaptic, immunological) prior to significant disease which are important to inform targets for translational research.

Data-driven analysis of transcriptomes through gene co-expression networks revealed two modules, denoted turquoise and lightyellow, that highlighted a molecular separation between normal age-related changes and changes related to AD-relevant biomarkers (Figure 3). While both modules were enriched for immune response, this enrichment was more significant in the turquoise ($p = 1.8 \times 10^{-49}$) than the lightyellow ($p = 3.7 \times 10^{-3}$) module (Table SB3). This suggests a more focused immune component in the lightyellow module, led by cytokine signaling (Figure 3C) and often co-annotated to lipid metabolism (Figure 3D). Furthermore, the lightyellow module was much more correlated with circulating cytokines and NfL, while the turquoise module was linked to more general IBA1 and GFAP markers (Figure 3B). These results suggest a signature for AD-related transcriptomic changes (the lightyellow module) that is distinct from usual brain aging (the turquoise module) and driven by diet in LOAD mice.

Though no deficits in hippocampal spatial working memory as measured by the spontaneous alternation task were observed in LOAD2 on either control or HFD, (Figure 1), aged LOAD2 mice demonstrated mild deficits in a pattern separation task relative to age-matched WT controls. Interestingly, across two separate cohorts, advanced aged mice conditioned on a HFD either from 2 months of age or from 6+ months of age failed to meet learning criteria with daily performance at or below chance levels (Figure 8 and Figure S7). Regardless, for aged WT and LOAD2 mice maintained on control diet, results from daily assessments on task acquisition reveal modest cognitive impairments in LOAD2 relative to WT. While modest, these cognitive deficits are further strengthened by the proteomic analysis of LOAD2 mice revealing alterations in synaptic signaling. While we were not able to conduct additional cognitive tests in this advanced aged cohort due to attrition and eventual mortality, as subjects aged to 24 months by the conclusion of testing, these data indicate that translational touchscreen tests may be more sensitive for detecting more specific cognitive domains than traditional single day behavioral tests in mice that have been historically used for assessing cognition.

Commensurate with the cytokines and multi-omic (Figure 3B) associations, cerebral perfusion, and metabolism via uncoupling analysis revealed a sexually dimorphic dysregulation with age and genotype (Figure 7,B). Importantly, the addition of a HFD in LOAD1 mice, resulted in Type 1 uncoupling (i.e., reductions in glycolysis and compensatory hyperemia), consistent with a cytokine (i.e., TNFα, IL-1β, IL-6, and/or IL-12)[26–29] driven down regulation of insulin receptors,[27] which have been shown to result in a reduction in neuronal glucose uptake

via GLUT transporters.[28–30] Importantly, these data closely parallel the Type 2 diabetic phenotype[31,32] with reactive hyperemia via activation of eNOS.[33]

To further explore the impact of environment on gene and sex, analysis of neurovascular uncoupling was performed to assess the degree of regional metabolic dysregulation in LOAD2 mice. Unlike the base model, LOAD2+HFD at 12 months resulted in a Type 2 neurovascular uncoupled phenotype (i.e., increased glycolysis and reduced perfusion) which was only observed in female mice. These data align with cytokines (i.e., TNFα, IL-2) and immunopathology changes (Figure 2,5) at this age, and are consistent with previous reports of cytokine driven astrocytic proliferation and GLUT1 expression.[34] By contrast, aging of LOAD2 mice to 18 months in the presence of HFD, resulted in whole brain increases in both perfusion and metabolism in nearly all brain regions studies. Importantly, these changes were observed in both sexes, and was consistent with reports of prodromal[35–38] and hyperemia[39] observed in clinical patients, suggesting that this model recapitulates the earliest manifestations of LOAD onset.

While there was robust cross-cohort and cross-laboratory replicability for plasma cytokines irrespective of the different laboratory environments, we observed divergent results for plasma Aβ for cohort 2 (Figure 5D,E) versus cohorts 4 and 5 (Figure 8J,K and Figure S7J,K). Two major factors may contribute to these differences beyond the different laboratory environments: (1) plasma Aβ was analyzed from anesthetized subjects during terminal procedures for cohort 2 whereas cohorts 4 and 5 were longitudinally sampled in non-anesthetized mice; and (2) cohorts 4 and 5 were subjected to periods of food restriction which was not a factor for cohort 2. It is well documented that variations in plasma Aβ are influenced by environmental factors including stress.[40] Despite the cross-lab variability for Aβ, irrespective of transient stressors, TNFα levels were sustained consistently across cohorts and align with transcriptomic and proteomic data which demonstrates the robustness of the LOAD2 × age × HFD model for preclinical studies of therapeutic interventions independent of amyloid.

Collectively, the data presented here suggest that LOAD2+HFD mice, particularly females, present with early stages of LOAD by 18 months of age. We were unable to determine whether aging LOAD2+HFD further would have further enhanced their LOAD-relevant phenotypes as LOAD2 or control mice fed the HFD showed increased incidence of tumors when aged beyond 18 months of age. Interestingly, LOAD2+CD mice aged to 24 months did not show as severe phenotypes as 18 months old LOAD2+HFD, highlighting the significance of chronic exposure to HFD in this model. Alternative milder diets are being tested that may recapitulate the LOAD-relevant phenotypes without the presence of tumors and attrition.

Including appropriate controls becomes challenging as the complexity of models increases. Here, we chose to use LOAD1 (a LOAD2 precursor) that we had previously phenotyped,[8] and B6 mice in some assays. Selecting LOAD1 as the primary control allowed us to segregate the hAβ allele through intercrossing LOAD1.App$^{hA\beta/+}$ mice providing littermate LOAD1 and LOAD2 controls (see methods). However, to understand the contributions of specific alleles to the phenotypes observed in LOAD2+HFD, it will be necessary to test additional single and double allele mice.

New generation models, based on combining genetic and environmental risk factors, are complementary to widely used transgenic and knock-in amyloid and tau models.[41–45] The majority of research to date has been focused on amyloid- or tau-dependent changes. As alternatives, LOAD2+HFD, and future models created by MODEL-AD, can be used to determine amyloid- and tau-independent processes that are likely occurring very early in disease, and test potential therapeutic approaches. Ultimately, the field requires an array of models that present with all aspects of LOAD to maximize the chances of developing effective therapies to treat this complex disease.

In summary, we present LOAD2+HFD, a model that incorporates genetic risk × aging that is exacerbated by an environmental risk factor. These include aspects of neuroinflammation with mild cognitive impairment independent of significant amyloid accumulation and prior to frank neuropathology. Multi-omic analysis revealed molecular signatures implicating key mechanisms such as synaptic signaling deficits that correspond to the impaired albeit modest cognitive phenotype observed. Importantly, translational measures of blood and imaging biomarkers position the LOAD2 model as an important model system for studying aspects of early progression of LOAD including for preclinical drug testing in a prophylactic approach prior to significant disease onset in which the drug's mechanism of action is matched for in vivo target engagement studies for the presence of the target protein based on proteomic and/or transcriptomic analysis.

AUTHOR CONTRIBUTIONS

Kevin P. Kotredes and Ravi S. Pandey, Gareth R. Howell and Adrian L. Oblak contributed to the study design and wrote the manuscript. Kathryn A. Haynes, Stacey J. Sukoff Rizzo, Adrian L. Oblak, Gregory W. Carter and Paul R. Territo conducted the data analysis and contributed to data interpretation. Kathryn A. Haynes, Sean-Paul Williams, Diogo Francisco S. Santos, Nicholas Heaton, Cynthia M. Ingraham, Christopher Lloyd, and Nian Wang conducted experiments and analyzed data. Gareth R. Howell, Adrian L. Oblak, Gregory W. Carter, Stacey J. Sukoff Rizzo, and Paul R. Territo oversaw the study. All the authors contributed to this article and approved the submitted version.

ACKNOWLEDGMENTS

The results published here are in whole or in part based on data obtained from the AD Knowledge Portal (https://adknowledgeportal.org). Study data were provided by the Rush Alzheimer's Disease Center, Rush University Medical Center, Chicago. Data collection was supported through funding by NIA grants P30AG10161 (ROS), R01AG15819 (ROSMAP; genomics and RNAseq), R01AG17917 (MAP), R01AG36836 (RNAseq), the Illinois Department of Public Health (ROSMAP), and the Translational Genomics Research Institute (genomic). Additional phenotypic data can be requested at www.radc.rush.edu. Mount Sinai Brain Bank data were generated from *post mortem* brain tissue collected through the Mount Sinai VA Medical Center Brain Bank and were provided by Dr. Eric Schadt from Mount Sinai

School of Medicine. The Mayo RNAseq study data was led by Nilüfer Ertekin-Taner, Mayo Clinic, Jacksonville, FL as part of the multi-PI U01 AG046139 (MPIs Golde, Ertekin-Taner, Younkin, Price). Samples were provided from the following sources: The Mayo Clinic Brain Bank. Data collection was supported through funding by NIA grants P50 AG016574, R01 AG032990, U01 AG046139, R01 AG018023, U01 AG006576, U01 AG006786, R01 AG025711, R01 AG017216, R01 AG003949, NINDS grant R01 NS080820, CurePSP Foundation, and support from Mayo Foundation. Study data includes samples collected through the Sun Health Research Institute Brain and Body Donation Program of Sun City, Arizona. The Brain and Body Donation Program was supported by the National Institute of Neurological Disorders and Stroke (U24 NS072026 National Brain and Tissue Resource for Parkinson's Disease and Related Disorders), the National Institute on Aging (P30 AG19610 Arizona Alzheimer's Disease Core Center), the Arizona Department of Health Services (contract 211002, Arizona Alzheimer's Research Center), the Arizona Biomedical Research Commission (contracts 4001, 0011, 05-901 and 1001 to the Arizona Parkinson's Disease Consortium), and the Michael J. Fox Foundation for Parkinson's Research. The authors are grateful for the technical support of the IUSM Biomarker Core. The authors are grateful for the technical support of the University of Pittsburgh Preclinical Phenotyping Core facility as well as the following research staff: Gabi Little, Jason Hart, Aman Reddy, Umesh Nepali, Jenny Willis, and Amber Sanders. The MODEL-AD Center was supported through funding by NIA grant U54AG054345. GH was supported by the Diana Davis Spencer Endowed Chair Research and GC was supported by the Bernard and Lusia Milch Endowed Chair. NW was supported by NINDS grant R01NS125020.

CONFLICT OF INTEREST STATEMENT

The authors declare that this research was conducted in the absence of any commercial or financial relationships that could be construed as a potential conflict of interest. Author disclosures are available in the supporting information.

DATA AVAILABILITY STATEMENT

The MODEL-AD data sets are available via the AD Knowledge Portal (https://adknowledgeportal.org). The AD Knowledge Portal is a platform for accessing data, analyses, and tools generated by the Accelerating Medicines Partnership (AMP-AD) Target Discovery Program and other National Institute on Aging (NIA)-supported programs to enable open-science practices and accelerate translational learning. The data, analyses, and tools are shared early in the research cycle without a publication embargo on secondary use. Data is available for general research use according to the following requirements for data access and data attribution (https://adknowledgeportal.org/DataAccess/Instructions). For access to content described in this manuscript, see: https://doi.org/10.7303/syn53128146.

ETHICS STATEMENT

All animal studies were reviewed and approved by the Indiana University Institutional Animal Care and Use Committee (IACUC), The University of Pittsburgh IACUC, and The Jackson Laboratory Animal Use Committee.

REFERENCES

1. Baumgart M, Snyder HM, Carrillo MC, Fazio S, Kim H, Johns H. Summary of the evidence on modifiable risk factors for cognitive decline and dementia: a population-based perspective. *Alzheimers Dement*. 2015;11(6):718-726. doi:10.1016/j.jalz.2015.05.016
2. Boyd RJ, Avramopoulos D, Jantzie LL, McCallion AS. Neuroinflammation represents a common theme amongst genetic and environmental risk factors for Alzheimer and Parkinson diseases. *J Neuroinflammation*. 2022;19(1):223. doi:10.1186/s12974-022-02584-x
3. Solfrizzi V, Panza F, Frisardi V, et al. Diet and Alzheimer's disease risk factors or prevention: the current evidence. *Expert Rev Neurother*. 2011;11(5):677-708. doi:10.1586/ern.11.56
4. Biogen. FDA approves updated ADUHELM™ Prescribing Information to Emphasize Population Studied in Clinical Trials. Biogen. 2021. Available from: https://investors.biogen.com/news-releases/news-release-details/fda-approves-updated-aduhelmtm-prescribing-information-emphasize
5. FDA. FDA Converts Novel Alzheimer's Disease Treatment to Traditional Approval. FDA. 2023. Available from: https://www.fda.gov/news-events/press-announcements/fda-converts-novel-alzheimers-disease-treatment-traditional-approval
6. Oblak AL, Forner S, Territo PR, et al, and The M-A, Consortium. Model organism development and evaluation for late-onset Alzheimer's disease: MODEL-AD. *Alzheimers Dement*. 2020;6(1):e12110. doi:10.1002/trc2.12110
7. Foley KE, Hewes AA, Garceau DT, et al. The APOE (epsilon3/epsilon4) genotype drives distinct gene signatures in the cortex of young mice. *Front Aging Neurosci*. 2022;14:838436. doi:10.3389/fnagi.2022.838436
8. Kotredes KP, Oblak AL, Pandey RS, et al. Uncovering disease mechanisms in a novel mouse model expressing humanized APOEε4 and Trem2*R47H. *Front Aging Neurosci*. 2021;13:735524.
9. Morris MC, Evans DA, Bienias JL, et al. Dietary fats and the risk of incident Alzheimer disease. *Arch Neurol*. 2003;60(2):194-200. doi:10.1001/archneur.60.2.194
10. Oblak AL, Kotredes KP, Pandey RS, et al. Plcg2(M28L) interacts with high fat/high sugar diet to accelerate Alzheimer's disease-relevant phenotypes in mice. *Front Aging Neurosci*. 2022;14:886575. doi:10.3389/fnagi.2022.886575
11. Sukoff Rizzo SJ, Anderson LC et al. Assessing healthspan and lifespan measures in aging mice: optimization of testing protocols, replicability, and rater reliability. *Curr Protoc Mouse Biol*. 2018;8(2):e45. doi:10.1002/cpmo.45
12. Backstrom D, Linder J, Jakobson Mo S, et al. NfL as a biomarker for neurodegeneration and survival in Parkinson disease. *Neurology*. 2020;95(7):e827-e838. doi:10.1212/WNL.0000000000010084
13. Langfelder P, Horvath S. WGCNA: an R package for weighted correlation network analysis. *BMC Bioinformatics*. 2008;9:559. doi:10.1186/1471-2105-9-559
14. Cary GA, Wiley JC, Gockley J, et al. The emory-sage SGCT-ADC. Genetic and multi-omic risk assessment of Alzheimer's disease implicates core associated biological domains. *medRxiv*. 2022. doi:10.1101/2022.12.15.22283478
15. Johnson ECB, Carter EK, Dammer EB, et al. Large-scale deep multilayer analysis of Alzheimer's disease brain reveals strong proteomic disease-related changes not observed at the RNA level. *Nat Neurosci*. 2022;25(2):213-225. doi:10.1038/s41593-021-00999-y
16. Buscher N, van Dorsselaer P, Steckler T, Talpos JC. Evaluating aged mice in three touchscreen tests that differ in visual demands: impaired cognitive function and impaired visual abilities. *Behav Brain Res*. 2017;333:142-149. doi:10.1016/j.bbr.2017.06.053

17. Oomen CA, Hvoslef-Eide M, Heath CJ, et al. The touchscreen operant platform for testing working memory and pattern separation in rats and mice. *Nat Protoc*. 2013;8(10):2006-2021. doi:10.1038/nprot.2013.124
18. Ano Y, Nakayama H. Preventive effects of dairy products on dementia and the underlying mechanisms. *Int J Mol Sci*. 2018;19(7):1927. doi:10.3390/ijms19071927
19. Li Y, Zhang ZH, Huang SL, et al. Whey protein powder with milk fat globule membrane attenuates Alzheimer's disease pathology in 3xTg-AD mice by modulating neuroinflammation through the peroxisome proliferator-activated receptor gamma signaling pathway. *J Dairy Sci*. 2023;106(8):5253-5265. doi:10.3168/jds.2023-23254
20. Min LJ, Kobayashi Y, Mogi M, et al. Administration of bovine casein-derived peptide prevents cognitive decline in Alzheimer disease model mice. *PLoS One*. 2017;12(2):e0171515. doi:10.1371/journal.pone.0171515
21. Urai AE, Aguillon-Rodriguez V, Laranjeira IC, et al. Citric acid water as an alternative to water restriction for high-yield mouse behavior. *eNeuro*. 2021;8(1): ENEURO.0230-20.2020. doi:10.1523/ENEURO.0230-20.2020
22. Milind N, Preuss C, Haber A, et al. Transcriptomic stratification of late-onset Alzheimer's cases reveals novel genetic modifiers of disease pathology. *PLoS Genet*. 2020;16(6):e1008775. doi:10.1371/journal.pgen.1008775
23. Mukherjee S, Heath L, Preuss C, et al. Molecular estimation of neurodegeneration pseudotime in older brains. *Nat Commun*. 2020;11(1):5781. doi:10.1038/s41467-020-19622-y
24. Naj AC, Schellenberg GD. Genomic variants, genes, and pathways of Alzheimer's disease: an overview. *Am J Med Genet B Neuropsychiatr Genet*. 2017;174(1):5-26. doi:10.1002/ajmg.b.32499
25. Verheijen J, Sleegers K. Understanding Alzheimer disease at the interface between genetics and transcriptomics. *Trends Genet*. 2018;34(6):434-447. doi:10.1016/j.tig.2018.02.007
26. Bennett DA. Mixed pathologies and neural reserve: implications of complexity for Alzheimer disease drug discovery. *PLoS Med*. 2017;14(3):e1002256. doi:10.1371/journal.pmed.1002256
27. Girouard H, Iadecola C. Neurovascular coupling in the normal brain and in hypertension, stroke, and Alzheimer disease. *J Appl Physiol (1985)*. 2006;100(1):328-335. doi:10.1152/japplphysiol.00966.2005
28. Kalaria RN, Erkinjuntti T. Small vessel disease and subcortical vascular dementia. *J Clin Neurol*. 2006;2(1):1-11. doi:10.3988/jcn.2006.2.1.1
29. Liu CC, Liu CC, Kanekiyo T, Xu H, Bu G. Apolipoprotein E and Alzheimer disease: risk, mechanisms and therapy. *Nat Rev Neurol*. 2013;9(2):106-118. doi:10.1038/nrneurol.2012.263
30. Bell RD, Winkler EA, Singh I, et al. Apolipoprotein E controls cerebrovascular integrity via cyclophilin A. *Nature*. 2012;485(7399):512-516. doi:10.1038/nature11087
31. Bomfim TR, Forny-Germano L, Sathler LB, et al. An anti-diabetes agent protects the mouse brain from defective insulin signaling caused by Alzheimer's disease- associated Abeta oligomers. *J Clin Invest*. 2012;122(4):1339-1353. doi:10.1172/JCI57256
32. Ferreira ST, Clarke JR, Bomfim TR, De Felice FG. Inflammation, defective insulin signaling, and neuronal dysfunction in Alzheimer's disease. *Alzheimers Dement*. 2014;10(Suppl1):S76-S83. doi:10.1016/j.jalz.2013.12.010
33. Yu J, deMuinck, ED, Zhuang Z, et al. Endothelial nitric oxide synthase is critical for ischemic remodeling, mural cell recruitment, and blood flow reserve. *Proc Natl Acad Sci U S A*. 2005;102(31):10999-11004. doi:10.1073/pnas.0501444102
34. Salvadó G, Milà-Alomà M, Shekari M, et al. Reactive astrogliosis is associated with higher cerebral glucose consumption in the early Alzheimer's continuum. *Eur J Nucl Med Mol Imaging*. 2022;49(13):4567-4579. doi:10.1007/s00259-022-05897-4
35. Ashraf A, Fan Z, Brooks DJ, Edison P. Cortical hypermetabolism in MCI subjects: a compensatory mechanism? *Eur J Nucl Med Mol Imaging*. 2015;42(3):447-458. doi:10.1007/s00259-014-2919-z
36. Rubinski A, Franzmeier N, Neitzel J. Ewers M. FDG-PET hypermetabolism is associated with higher tau-PET in mild cognitive impairment at low amyloid-PET levels. *Alzheimers Res Ther*. 2020;12(1):133. doi:10.1186/s13195-020-00702-6
37. Willette AA, Modanlo N, Kapogiannis D. Insulin resistance predicts medial temporal hypermetabolism in mild cognitive impairment conversion to Alzheimer disease. *Diabetes*. 2015;64(6):1933-1940. doi:10.2337/db14-1507
38. Yu L, Jin J, Xu Y, Zhu X. Aberrant energy metabolism in Alzheimer's disease. *J Transl Int Med*. 2022;10(3):197-206. doi:10.2478/jtim-2022-0024
39. Thomas KR, Osuna JR, Weigand AJ, et al. Regional hyperperfusion in older adults with objectively-defined subtle cognitive decline. *J Cereb Blood Flow Metab*. 2021;41(5):1001-1012. doi:10.1177/0271678X20935171
40. Dong H, Csernansky JG. Effects of stress and stress hormones on amyloid-beta protein and plaque deposition. *J Alzheimers Dis*. 2009;18(2):459-469. doi:10.3233/jad-2009-1152
41. Oakley H, Cole SL, Logan S, et al. Intraneuronal beta-amyloid aggregates, neurodegeneration, and neuron loss in transgenic mice with five familial Alzheimer's disease mutations: potential factors in amyloid plaque formation. *J Neurosci*. 2006;26(40):10129-10140. doi:10.1523/JNEUROSCI.1202-06.2006
42. Oblak AL, Lin PB, Kotredes KP, et al. Comprehensive evaluation of the 5XFAD mouse model for preclinical testing applications: a MODEL-AD study. *Front Aging Neurosci*. 2021;13:713726. doi:10.3389/fnagi.2021.713726
43. Saito T, Matsuba Y, Mihira N, et al. Single App knock-in mouse models of Alzheimer's disease. *Nat Neurosci*. 2014;17(5):661-663. doi:10.1038/nn.3697
44. Xia D, Lianoglou S, Sandmann T, et al. Novel App knock-in mouse model shows key features of amyloid pathology and reveals profound metabolic dysregulation of microglia. *Mol Neurodegener*. 2022;17(1):41. doi:10.1186/s13024-022-00547-7
45. Yoshiyama Y, Higuchi M, Zhang B, et al. Synapse loss and microglial activation precede tangles in a P301S tauopathy mouse model. *Neuron*. 2007;53(3):337-351. doi:10.1016/j.neuron.2007.01.010

SUPPORTING INFORMATION

Additional supporting information can be found online in the Supporting Information section at the end of this article.

How to cite this article: Kotredes KP, Pandey RS, Persohn S, et al. Characterizing molecular and synaptic signatures in mouse models of late-onset Alzheimer's disease independent of amyloid and tau pathology. *Alzheimer's Dement*. 2024;20:4126–4146. https://doi.org/10.1002/alz.13828